ELECTROCHEMISTRY

Metal-organic frameworks and their derived materials for electrochemical energy storage and conversion: Promises and challenges

Hao Bin Wu[1] and Xiong Wen (David) Lou[1,2]*

In addition to their conventional uses, metal-organic frameworks (MOFs) have recently emerged as an interesting class of functional materials and precursors of inorganic materials for electrochemical energy storage and conversion technologies. This class of MOF-related materials can be broadly categorized into two groups: pristine MOF-based materials and MOF-derived functional materials. Although the diversity in composition and structure leads to diverse and tunable functionalities of MOF-based materials, it appears that much more effort in this emerging field is devoted to synthesizing MOF-derived materials for electrochemical applications. This is in view of two main drawbacks of MOF-based materials: the low conductivity nature and the stability issue. On the contrary, MOF-derived synthesis strategies have substantial advantages in controlling the composition and structure of MOF-derived materials. From this perspective, we review some emerging applications of both groups of MOF-related materials as electrode materials for rechargeable batteries and electrochemical capacitors, efficient electrocatalysts, and even electrolytes for electrochemical devices. By highlighting the advantages and challenges of each class of materials for different applications, we hope to shed some light on the future development of this highly exciting area.

INTRODUCTION

Renewable energy sources, such as solar and wind power, are taking up a growing portion of total energy consumption of human society. Owing to the intermittent and fluctuating power output of these energy sources, electrochemical energy storage and conversion technologies, such as rechargeable batteries, electrochemical capacitors, electrolyzers, and fuel cells, are playing key roles toward efficient and sustainable energy utilization (*1*, *2*). For example, electricity generated from solar and wind power can be efficiently stored in and released from rechargeable batteries and electrochemical capacitors, or converted into fuels by electrolyzers and further regenerated by fuel cells. Despite their different working principles, these electrochemical devices include the following key functional components (*3*): two electrodes (cathode and anode), where the major electrochemical processes take place, such as charge storage in batteries/capacitors and electrocatalytic reactions in electrolyzers/fuel cells, and an electrolyte that allows the transport of ions and blocks electronic conduction to complete the electric circuit. In principle, the physical (for example, electronic and ionic conductivity) and electrochemical (for example, redox and catalytic activity) properties of functional materials used in these components govern the performance of devices. Therefore, seeking better materials has been a primary quest for the development of future electrochemical energy–related technologies.

As a relatively young but quickly growing family of porous materials, metal-organic frameworks (MOFs) have generated a tremendous amount of interest from researchers in widespread areas (*4*, *5*). With different metal-containing nodes, organic ligands, and connectivity, more than 20,000 different MOFs have been reported by the year 2013 and the number continues to grow (*4*). The composition and pore structure of MOFs can be modulated by tuning the precursors and synthetic conditions or by postsynthetic modifications. In addition, MOFs can be synthesized as nanoparticles and can also form nanocomposites with additional active components. The diversity of composition and structure leads to diverse and tunable functionalities of MOFs. The remarkably high porosity and surface area of MOFs are especially suitable for applications involving storage and interaction with guest species (for example, gas storage/separation and catalysis) (*4*, *6*). These features also trigger extensive research interests to explore the adaptation of MOF-related materials for electrochemical energy storage and conversion (*7*–*10*). Similar to conventional inorganic materials, MOFs containing redox-active metal centers, typically first-row transition metals (Fe, Co, Ni, Mn, etc.), are of particular interest for delivering electrochemical activity. Compared with both conventional inorganic and polymeric functional materials, MOFs might inherit their advantages (for example, electrochemically active metal centers and organic functional groups). Some additional benefits are also apparent, such as fully accessible organic molecule–coordinated metal sites and easily tunable pore structures. By tuning the metal and organic constituent components and/or constructing composites, MOFs have been successfully demonstrated as electrode materials for rechargeable batteries and electrochemical capacitors, efficient electrocatalysts for fuel production and utilization, and even electrolytes for electrochemical devices (*9*). Alternatively, to overcome the limitations of insufficient electronic conductivity and chemical stability of most pristine MOFs, converting MOFs into metal compounds, carbonaceous materials, or their composites has also been extensively explored (*11*–*15*). These MOF-derived functional materials usually exhibit remarkable advantages originating from their microstructures/nanostructures, showing great potential for energy-related technologies.

Development of MOF-related materials for electrochemical energy storage and conversion has been a rapidly expanding research area in the past decade. Several excellent reviews have summarized recent advances in this field mostly focusing on specific aspects, such as MOF-related materials for specific applications (for example, photocatalysis/electrocatalysis and energy storage devices) or functional/nanostructured

[1]School of Materials Science and Engineering, Zhejiang University, Hangzhou 310027, P. R. China. [2]School of Chemical and Biomedical Engineering, Nanyang Technological University, 62 Nanyang Drive, Singapore 637459, Singapore.
*Corresponding author. Email: xwlou@ntu.edu.sg

materials derived from MOFs (*8*–*10*, *13*–*19*). From the perspective of materials science, all these aspects are interrelated and essentially deal with the creation and modulation of electrochemical properties for energy-related applications. Therefore, an overview of this exciting research field is highly desirable. In this perspective, we aim to provide an overview for this highly interdisciplinary area and discuss the significant breakthroughs that MOF-related materials have brought to the field of electrochemical energy storage and conversion (Fig. 1). Some coordination polymers and open-framework materials that might not be strictly defined as MOFs are also included for discussion. In particular, we will discuss how different functionalities are realized from the perspective of materials design and synthesis. On the basis of their chemical nature, MOF-related materials can be categorized into two groups: MOF-based materials refer to pristine/modified MOFs or composites that contain MOF moieties, and MOF-derived materials include various inorganic functional materials that are synthesized using MOFs as precursors and/or templates. These MOF-related functional materials offer unprecedented opportunities to both existing and emerging energy-related technologies. By reviewing recent advances, we hope to provide some future directions for the development of MOF-related functional materials, especially toward renewable energy–related applications.

MOF-BASED MATERIALS

Electrochemical charge storage

Rechargeable batteries and electrochemical capacitors are two primary types of electrochemical energy storage devices. Batteries, such as lithium-ion and sodium-ion batteries (LIBs and SIBs), rely on reversible shuttling of lithium/sodium ions between two electrodes, offering high energy density and moderate power density (*20*). In a typical LIB, Li^+ ions deintercalate from a cathode (for example, $LiCoO_2$), transport through an electrolyte, and intercalate into an anode (for example, graphite) when charging the cell, and this process reverses during discharging. In 2007, Férey and co-workers (*21*) reported the electrochemical lithium insertion in an iron-based MOF, MIL-53(Fe), with a limited specific capacity of 75 mAh g^{-1} based on the Fe^{III}/Fe^{II} redox couple. Similar lithium storage properties have been recently reported in MIL-101(Fe) with limited reversibility (*22*). In some cases, high reversible capacity can be obtained via possible conversion and/or alloying reactions at low potential, whereas detailed investigations would be necessary to reveal the mechanism (*23*, *24*).

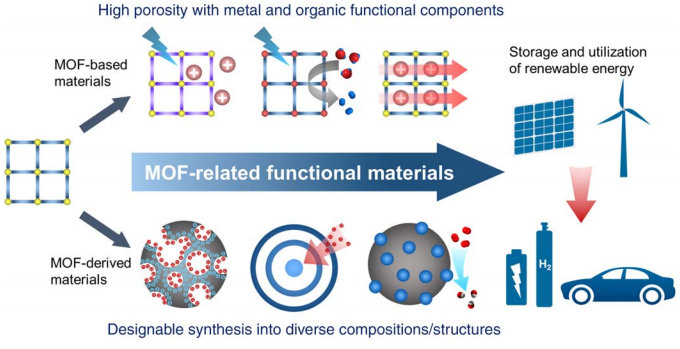

Fig. 1. Schematic of MOF-related materials for renewable energy. MOF-based materials with different functionalities by tuning the constituent components: (left to right) electrochemical charge storage, electrocatalytic generation of fuels, and ionic conductivity. MOF-derived materials with different compositions, structures, and functionalities: (left to right) porous carbon with electric double-layer capacitance, hollow structure for charge storage, and carbon-supported composite for electrocatalysis. These MOF-related functional materials enable the storage and utilization of electricity from renewable energy sources.

A feasible solution to increase the reversible capacity of MOFs is to introduce redox-active ligands, providing both cationic (metal centers) and anionic (ligands) redox activity. This was first exemplified by lithium storage in a two-dimensional (2D) MOF containing a redox-active bridging ligand (Fig. 2A) (*25*). The charge-discharge voltage profiles of the resulting MOF exhibit two distinct stages (Fig. 2B): a high-potential plateau attributed to the Cu^{II}/Cu^{I} redox couple and a low-potential plateau originated from anthraquinone groups in the ligands. With a total transfer of three electrons per formula unit, a high specific capacity of 147 mAh g^{-1} was reported, despite some gradual capacity fading (Fig. 2C). A similar strategy has been adopted to fabricate MOF-based cathode materials for SIBs (*26*).

Prussian blue and its analogues, with a general formula of $A_xM[M'(CN)_6]$ (A, mobile cations; M and M′, transition metal cations), appear as very promising open-framework materials for electrochemical ion insertion. Unlike the limited ion insertion in typical MOFs, two or even more alkaline cations, such as Li^+ and Na^+, can be accommodated per formula unit under optimized conditions (Fig. 2D), leading to high specific capacity (for example, about 170 mAh g^{-1} based on $Na_2Fe[Fe(CN)_6]$) with fast kinetics (*27*–*31*). Of particular interest is the reversible uptake of large cations, such as K^+ and Rb^+, or even multivalent cations (*32*), which is difficult for conventional inorganic compounds. This exceptional capability to host large guest molecules in open frameworks is further demonstrated by the oxidative insertion of anions in a Fe-based MOF, enabling the development of dual-ion batteries (*33*).

Electrochemical capacitors, also known as supercapacitors, store charge by either electrical double-layer capacitance or pseudocapacitance, and hence are able to deliver high power density and long life span (*20*). Double-layer capacitance refers to electrical charge storage by adsorption of ions at the interface between an electrode (typically porous carbon) and a liquid electrolyte without redox process. Pseudocapacitance, on the other hand, involves ultrafast redox reactions at the (near-)surface region or even in the bulk of an electrode (typically transition metal oxides). High surface area and redox-active metal centers of MOFs can potentially offer high double-layer capacitance and pseudocapacitance, respectively. To fabricate electrochemical capacitors, a series of 23 different MOFs in nanocrystalline form has been recently explored by Choi *et al.* (*34*) (Fig. 2E). As expected, the electrochemical performance (capacitance, cycle life, charge-discharge profiles, etc.) varies notably among different MOFs, revealing their composition/structure-dependent properties. The best-performing MOF delivers energy and power densities notably higher than those of the benchmark activated carbon (Fig. 2F).

The insulating nature of most reported MOFs appears to be a major obstacle for their electrochemical applications, especially for electrochemical capacitors with high power output. Adding a large amount of conductive additives or using thin-film electrodes could be adopted as compromised solutions (*25*, *34*). Meanwhile, developing MOFs with high electronic conductivity would address the issue on a fundamental basis (*35*). For example, Sheberla and co-workers (*36*) recently demonstrated that a nickel-based MOF, $Ni_3(HITP)_2$, with a high electronic conductivity over 5000 S m^{-1} and sufficient pore size for accommodating electrolyte species, could be used as an active material for electrochemical capacitors (Fig. 2, G and H). With a voltage window of 1.0 V, a symmetric electrochemical capacitor based on $Ni_3(HITP)_2$ exhibits a nearly ideal double-layer capacitive behavior (Fig. 2I). With an extended voltage

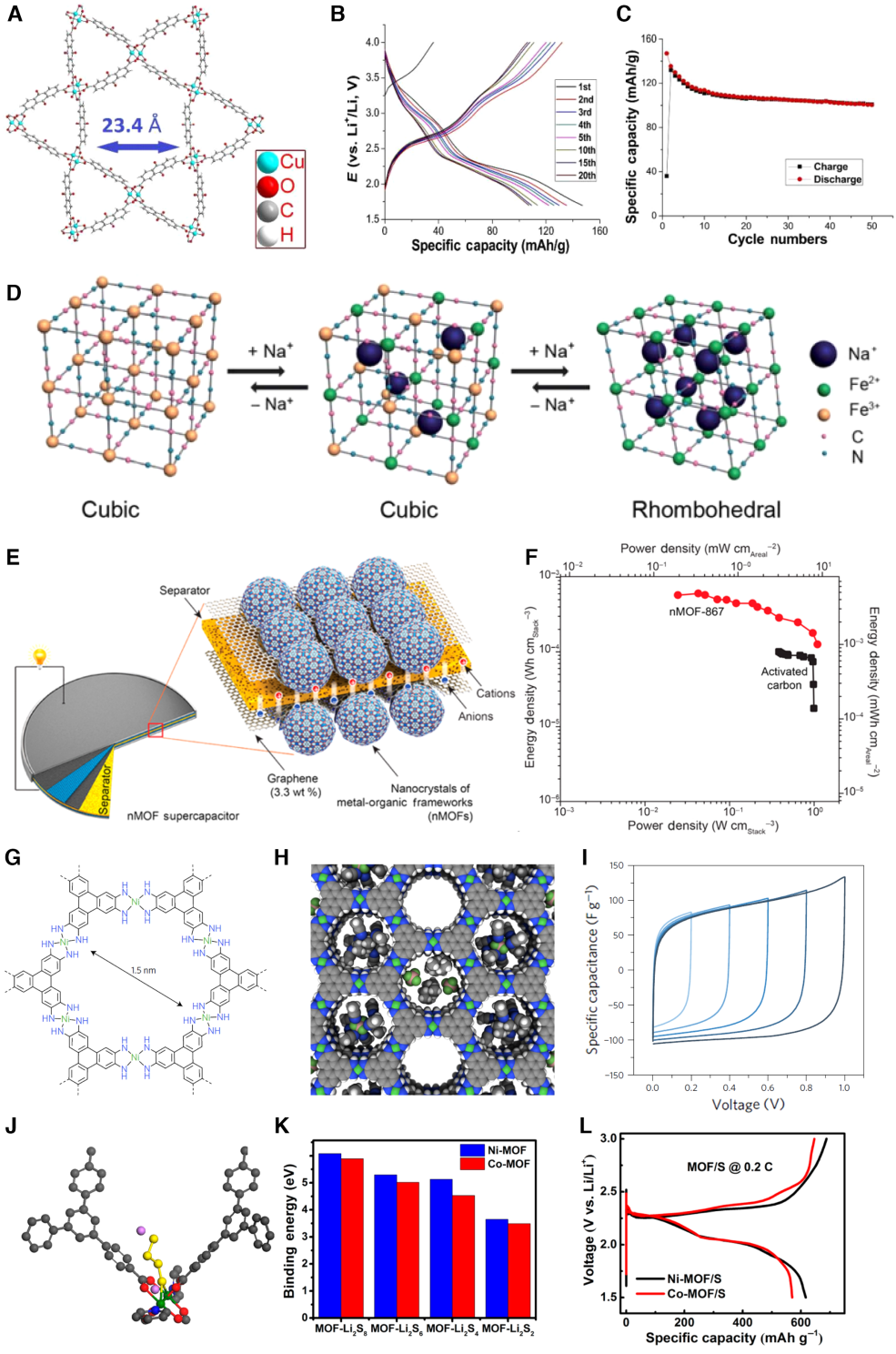

Fig. 2. MOF-related materials for charge storage. (**A** to **C**) A redox-active MOF Cu(2,7-anthraquinonedicarboxylate) [Cu(2,7-AQDC)] for lithium batteries: (A) structural schematic, (B) charge-discharge profiles, and (C) cycling performance [(A) to (C), adapted with permission from Zhang *et al*. (*25*)]. (**D**) Schematic of electrochemical Na storage in Prussian blue crystal [(D), adapted with permission from You *et al*. (*28*)]. (**E** and **F**) Electrochemical capacitors fabricated with nanocrystals of MOFs (nMOFs): (E) structure of nMOF electrochemical capacitor and (F) comparison of energy and power densities for electrochemical capacitors made from nMOF-867 and activated carbon [(E) and (F), adapted with permission from Choi *et al*. (*34*)]. (**G** to **I**) Electronic conductive MOF for electrochemical capacitors: structural schematics of (G) conductive MOF Ni_3(2,3,6,7,10,11-hexaiminotriphenylene)$_2$ [Ni_3(HITP)$_2$] and (H) electrolyte components in Ni_3(HITP)$_2$; (I) cyclic voltammetry at a scan rate of 10 mV s^{-1} at different cell voltages [(G) to (I), adapted with permission from Sheberla *et al*. (*36*)]. (**J** to **L**) MOFs as sulfur host for lithium-sulfur (Li-S) batteries: (J) schematic showing the interaction between polysulfides and MOF scaffold, (K) comparison of binding energy of lithium polysulfides to Ni-MOF or Co-MOF, and (L) charge-discharge profiles of MOF/S composite cathodes [(J) to (L), adapted with permission from Zheng *et al*. (*38*)].

window, a Faradaic process presumably attributed to quasi-reversible oxidation of $Ni_3(HITP)_2$ is observed, implying the possibility of introducing pseudocapacitance in MOF-based electrochemical capacitors.

MOF-based materials could also function as scaffolds to host active components, for example, O_2/Li_2O_2 in lithium-air batteries and S/Li_2S in Li-S batteries (*37*, *38*). Unlike porous carbon materials with relatively inert surfaces, the presence of open metal sites (OMSs) in many MOFs would interact with active species in electrodes and improve the electrochemical performance. Zheng *et al.* (*38*) reported a stable sulfur cathode based on a Ni-MOF/S composite. The strong binding between polysulfides (intermediates of reduced sulfur) and Ni^{II} centers of the Ni-MOF host plays an important role in preventing the loss of active materials from the electrode (Fig. 2J). This is further verified by a Co-MOF with identical structure but weaker interaction with polysulfides (Fig. 2K), which produces Co-MOF/S composite with lower specific capacity (Fig. 2L). In addition, the interaction between MOFs and sulfur species can be tuned by altering the OMSs or the pore structures (*39*, *40*). Thus, better sulfur hosts could be developed, combining theoretical prediction and experimental verification.

Electrocatalysis for energy conversion

Electrocatalysts are the central component of electrochemical energy conversion systems, which efficiently catalyze reactions to convert electricity into fuels for storage/transport or, in the opposite way, to regenerate electricity for on-site utilization (*2*). Specifically, electrochemical water splitting using electrolyzers produces hydrogen fuel by hydrogen evolution reaction (HER) coupled with oxygen evolution reaction (OER). Hydrocarbon fuels or other useful chemicals can be produced from carbon dioxide (CO_2) reduction, aiming for a carbon-neutral economy. In the meantime, electrochemical oxidation of fuels (for example, hydrogen for proton exchange membrane fuel cells) and oxygen reduction reaction (ORR) occur in fuel cells to generate electricity. Electrocatalysts are loaded on supports to form electrodes, allowing access of reactants and release of products in liquid and/or gas phases. An ideal electrocatalyst should exhibit features such as low overpotential during operation, high selectivity for desirable reactions, high durability, and low cost. Noble metals are highly efficient for many above-mentioned reactions (for example, platinum for HER and ORR). However, for large-scale deployment of these energy conversion technologies, low-cost noble metal–free catalysts are highly demanded (*41*).

MOFs can be considered as polymerized forms of molecular catalysts, offering highly exposed coordinated metal centers as active sites. For example, transition metal porphyrins, a class of efficient molecular catalysts, can be transformed to heterogeneous catalysts by incorporating into MOFs as linkers for ORR (Fig. 3A) (*42*) or CO_2 reduction (*43*). Metal nodes in MOFs with OMSs could also potentially serve as active sites for various electrocatalytic reactions (*44*–*46*). However, regardless of targeted reactions, adaptation of MOF-based materials as efficient electrocatalysts has been generally hampered by low electronic conductivity, limited accessibility of active sites, and insufficient chemical stability.

The emerging family of conductive MOFs also brings opportunities to the development of efficient electrocatalysts. The conductive $Ni_3(HITP)_2$ MOF (*36*) has been demonstrated as an active ORR electrocatalyst (Fig. 3B) (*45*). The nitrogen-coordinated Ni centers are structurally analogous to M-N_x (M = Fe, Co, Ni, etc.) units that have been actively explored as noble metal–free ORR catalysts (*47*). Despite the competitive ORR onset potential, the predominant two-electron reduction, rather than the more desirable four-electron reduction process observed for the $Ni_3(HITP)_2$ catalyst, suggests the need to develop more effective active centers. Meanwhile, thin films of cobalt-dithiolene–based MOFs with 1D or 2D structures have been explored as electrocatalysts for HER (*44*, *48*), where the combination of active cobalt-dithiolene sites, high electronic conductivity (*49*), and robust attachment to the electrode surface would contribute to the high activity.

To increase the amount of easily accessible active sites on the surface, the construction of 2D nanostructures has been demonstrated for MOF-based catalysts by Zhao and co-workers (*46*). The small thickness of 3.1 nm of ultrathin Ni-Co MOF nanosheets (NiCo-UMOFNs) corresponds to only four metal coordination layers (Fig. 3, C and D). With exposure of a large amount of OMSs on both surfaces and the coupling effect between Co and Ni, NiCo-UMOFNs exhibit an onset potential for OER notably lower than that of bulky and mono-metal counterparts (Fig. 3E). In another attempt to develop advanced OER electrocatalysts, paddle wheel–type Co-based clusters are bound to a highly stable Fe-based MOF by a delicately designed postsynthetic approach, delivering both high activity and good stability (*50*). Alternatively, Manna *et al.* (*51*) immobilized a mononuclear Co^{II} complex in the cavity of a MOF, producing an efficient OER electrocatalyst with a "ship-in-a-bottle" hybrid structure.

The stability issues of MOF-based electrocatalysts during operation in highly acidic or basic solutions should not be overlooked (*52*). In addition, the true structure of the catalyst surfaces generally remains uncertain, raising serious difficulties for mechanistic studies. As an example, a recent work (*53*) on a Co-based MOF (MAF-X27-Cl) as a candidate for OER catalysts reveals an in situ replacement of Cl^- ligands with OH^- in an alkaline electrolyte, producing a new MOF of MAF-X27-OH (Fig. 3F). The OER activity of MAF-X27-OH has been dramatically boosted by OH^- coordinated to the Co-based OMSs, with an electrocatalytic activity notably higher than that of $Co(OH)_2$ and Co_3O_4 (Fig. 3G). In addition, growing MOF catalysts directly on a conductive substrate can further improve the performance, highlighting the importance of electronic conduction.

Other than directly functioning as electrocatalysts, some MOFs can work as supporting components in electrocatalytic systems. As reported by Hod and co-workers (*54*), a Ni-S electrocatalyst for HER is electrodeposited on the conductive glass substrate (FTO) with an array of NU-1000 (a Zr-based MOF) rods. Although a flat layer of Ni-S is deposited on the substrate (Fig. 3H), rather than on the surface of NU-1000 rods, notably improved electrocatalytic activity has been observed in an acidic electrolyte compared with Ni-S deposited on a bare substrate (Fig. 3I). Considering the inactive nature of NU-1000 for HER, the authors reasoned that the high activity of the NU-1000/Ni-S hybrid system can be attributed to the promoted local proton delivery and/or transport (*54*). This work highlights the roles of MOFs as ionic conductors, which will be further discussed in detail in the following section.

Ionic conductors for electrolytes

Electrolytes allow facile transport of ions but not electrons, completing the electric circuit in electrochemical devices without direct short circuit between two electrodes (*3*). In batteries and electrochemical capacitors, liquid electrolytes composed of soluble salts and water/organic solvents are commonly used, whereas lithium-based batteries with solid electrolytes have been under active exploration. For fuel cells and electrolyzers, solid electrolytes (for example, proton-conducting Nafion) are widely used to block gases or other soluble reactants/products. The open-pore channels in MOFs imply potential ionic transport with high efficiency, and the insulating character of many MOFs becomes an advantage when applying MOFs for electrolytes. With proper materials design

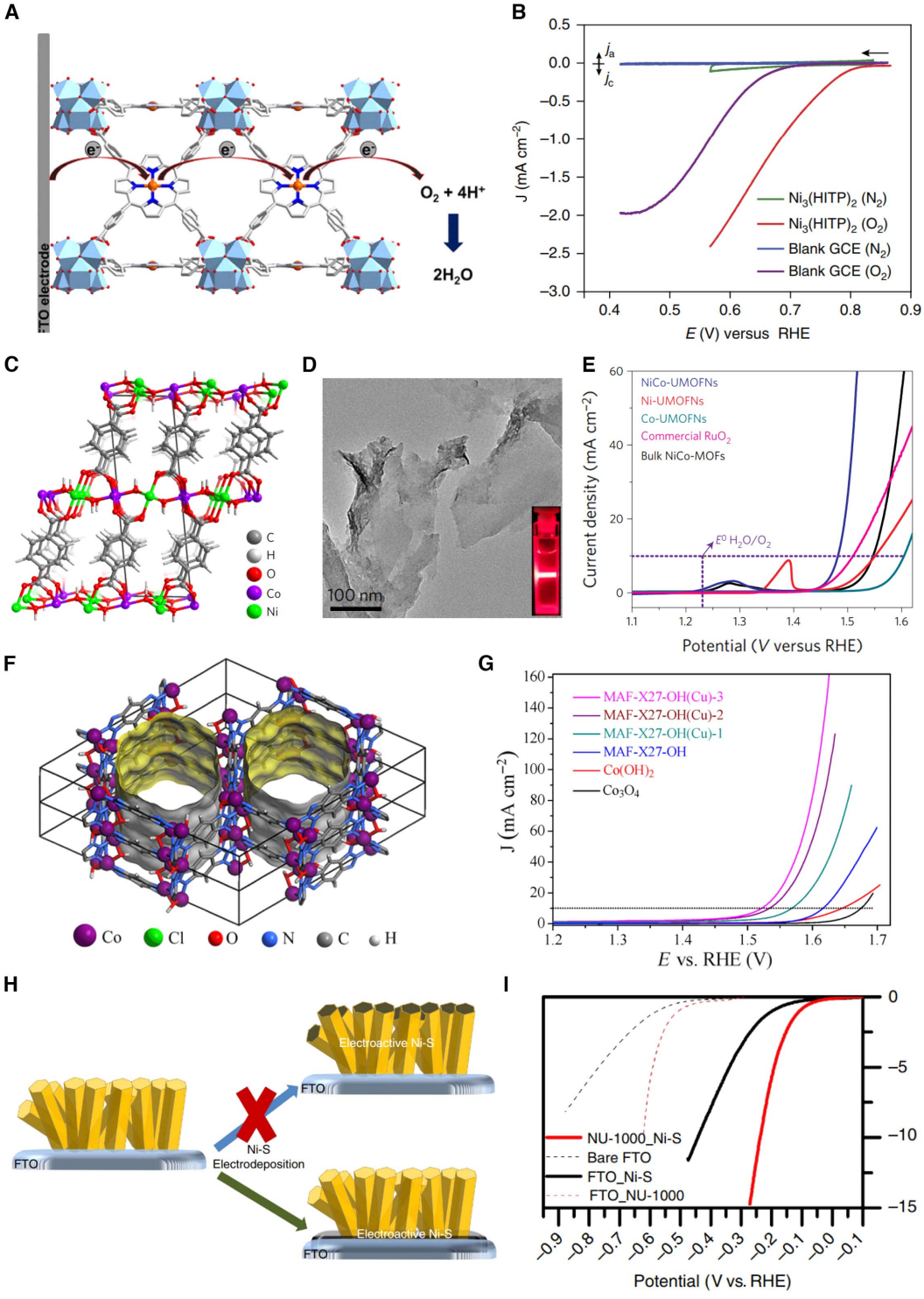

Fig. 3. MOF-related materials for electrocatalysis. (**A**) Schematic of a Zr-based MOF with Fe^{III} porphyrin linkers as a heterogeneous catalyst for ORR [(A), adapted with permission from Usov *et al.* (*42*)]. (**B**) Polarization curves of $Ni_3(HITP)_2$ under N_2 and O_2 atmosphere in 0.1 M KOH aqueous electrolyte at a scan rate of 5 mV s^{-1} and a rotation rate of 2000 rpm [(B), adapted with permission from Miner *et al.* (*45*)]. (**C** to **E**) UMOFNs as an electrocatalyst for OER: (C) crystal structure and (D) transmission electron microscopy (TEM) image of NiCo-UMOFNs and (E) polarization curves of various OER catalysts in O_2-saturated 1 M KOH solution at a scan rate of 5 mV s^{-1} [(C) to (E), adapted with permission from Zhao *et al.* (*46*)]. (**F** and **G**) A Co-based MOF, MAF-X27-OH, for OER: (F) structure of MAF-X27-OH and (G) polarization curves of various Co-based catalysts at pH = 14 [three MAF-X27-OH(Cu) samples refer to the MOF catalyst directly grown on the Cu substrate] [(F) and (G), adapted with permission from Lu *et al.* (*53*)]. (**H** and **I**) A Ni-S electrocatalyst deposited on the fluorine-doped tin oxide (FTO) substrate with an array of NU-1000 rods for HER: (H) schematic of the creation of NU-1000_Ni-S hybrid system and (I) polarization curves of various catalysts in 0.1 M HCl aqueous electrolyte [(H) and (I), adapted with permission from Hod *et al.* (*54*)]. GCE, glassy carbon electrodes; RHE, reversible hydrogen electrode.

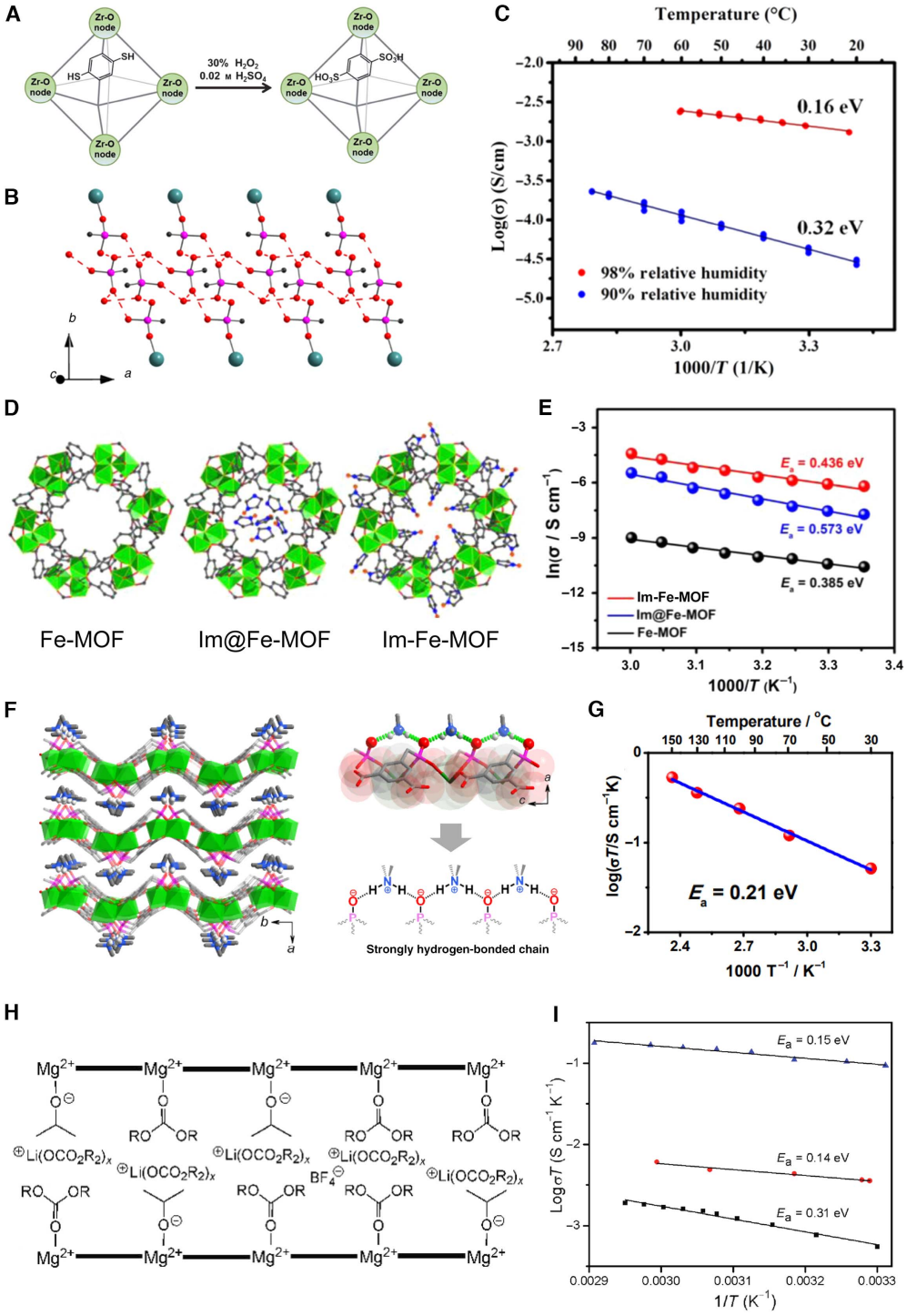

Fig. 4. MOF-related materials for ionic conduction. (**A**) Schematic of postsynthetic oxidation modification to synthesize UiO-66$(SO_3H)_2$ [(A), adapted with permission from Phang *et al*. (*58*)]. (**B** and **C**) PCMOF-5 with uncoordinated diprotic phosphonic acid groups for proton conduction: (B) 1D hydrogen-bonding array formed between phosphonic acid groups and free water molecules and (C) Arrhenius plots for PCMOF-5 at 90 and 98% RH [(B) and (C), adapted with permission from Taylor *et al*. (*60*)]. (**D** and **E**) A Fe-based MOF with imidazole for proton conduction: (D) structures of pristine Fe-MOF, imidazole physically absorbed in Fe-MOF (Im@Fe-MOF), and imidazole chemically coordinated in Fe-MOF (Im-Fe-MOF), and (E) their Arrhenius plots at 98% RH [(D) and (E), adapted with permission from Zhang *et al*. (*65*)]. (**F** and **G**) A layered anionic framework with interlayer-embedded counter cations for anhydrous proton conduction: (F) sandwich-type structure with cations $(Me_2NH_2)^+$ periodically aligned in the interlayers (left) and the strongly hydrogen-bonded chains (right) and (G) Arrhenius plot under anhydrous condition [(F) and (G), adapted with permission from Wei *et al*. (*66*)]. (**H** and **I**) A Mg-based MOF with lithium isopropoxide as a lithium-ion conductor: (H) schematic of the modified channel of Mg-based MOF and (I) Arrhenius plots of MOF with liquid electrolyte (black cubes), with lithium isopropoxide and solvent (red dots), and with both lithium isopropoxide and liquid electrolyte (blue triangles) [(H) and (I), adapted with permission from Wiers *et al*. (*71*)].

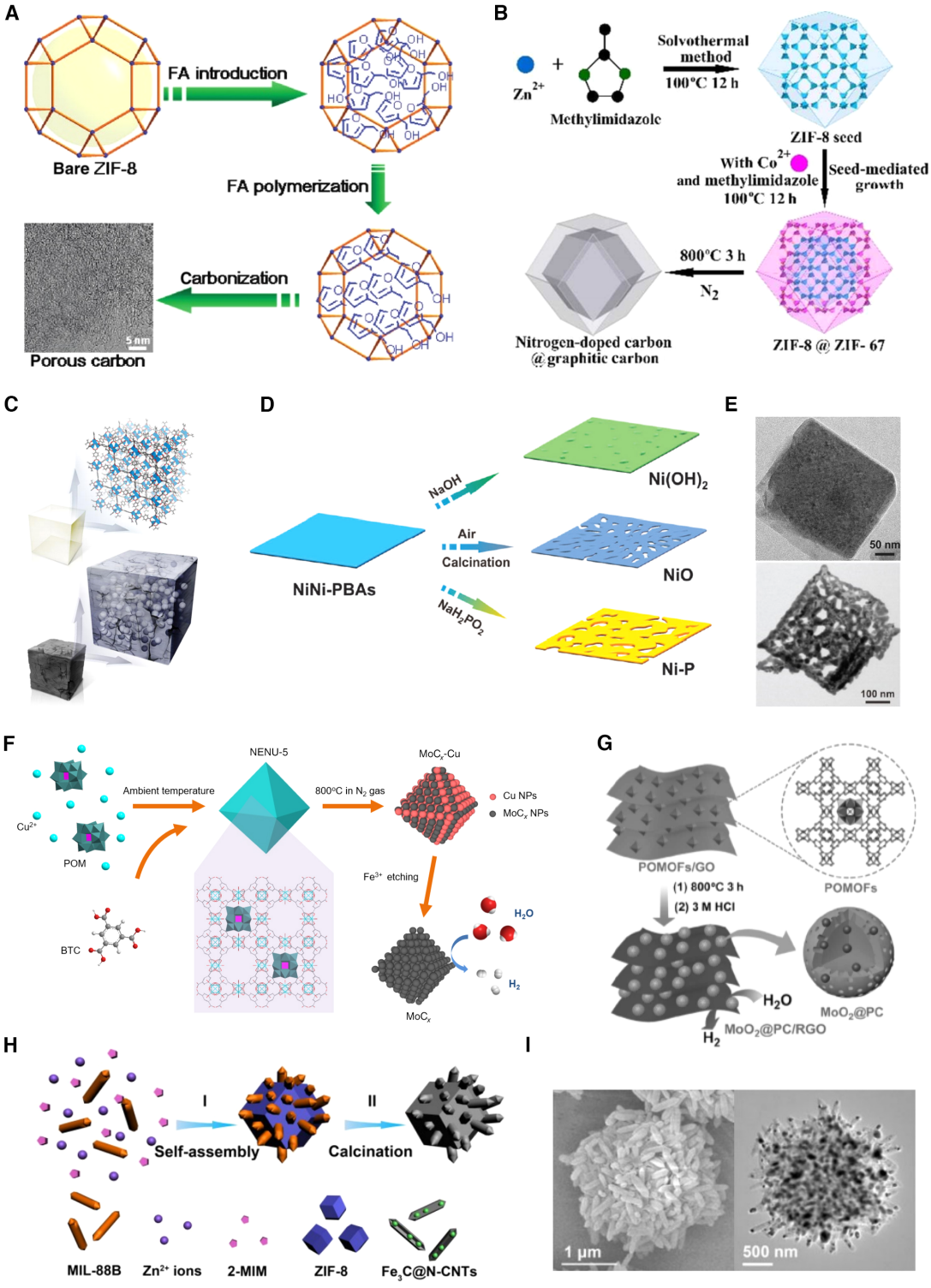

Fig. 5. Compositional control of MOF-derived materials. (**A**) Synthesis of porous carbon by carbonization of ZIF-8 with infiltrated furfuryl alcohol (FA) [(A), adapted with permission from Jiang *et al.* (*74*)]. (**B**) Synthesis of hybrid nanoporous carbon by carbonization of core-shell MOF particles [(B), adapted with permission from Tang *et al.* (*78*)]. (**C**) Synthesis of porous carbon-coated ZnO quantum dots by pyrolysis of IRMOF-1 [(C), adapted with permission from Yang *et al.* (*86*)]. (**D** and **E**) Various Ni-based inorganic compounds derived from NiNi-PBAs: (D) schematic of the synthesis strategy and (E) TEM images of the NiNi-PBAs (upper) and derived porous Ni-P (lower) [(D) and (E), adapted with permission from Yu *et al.* (*96*)]. (**F**) Synthesis of mesoporous MoC_x octahedral particles derived from NENU-5 [(F), adapted with permission from Wu *et al.* (*102*)]. (**G**) Synthesis of MoO_2-based composite (MoO_2@PC/RGO) from a MOF precursor containing POMs [(G), adapted with permission from Tang *et al.* (*103*)]. (**H** and **I**) A composite of Fe_3C@N-CNTs derived from a MOF-in-MOF composite: (H) schematic of the synthetic procedure and (I) microscope images of the composite precursor (left) and the derived Fe_3C@N-CNTs assemblies (right) [(H) and (I), adapted with permission from Guan *et al.* (*84*)].

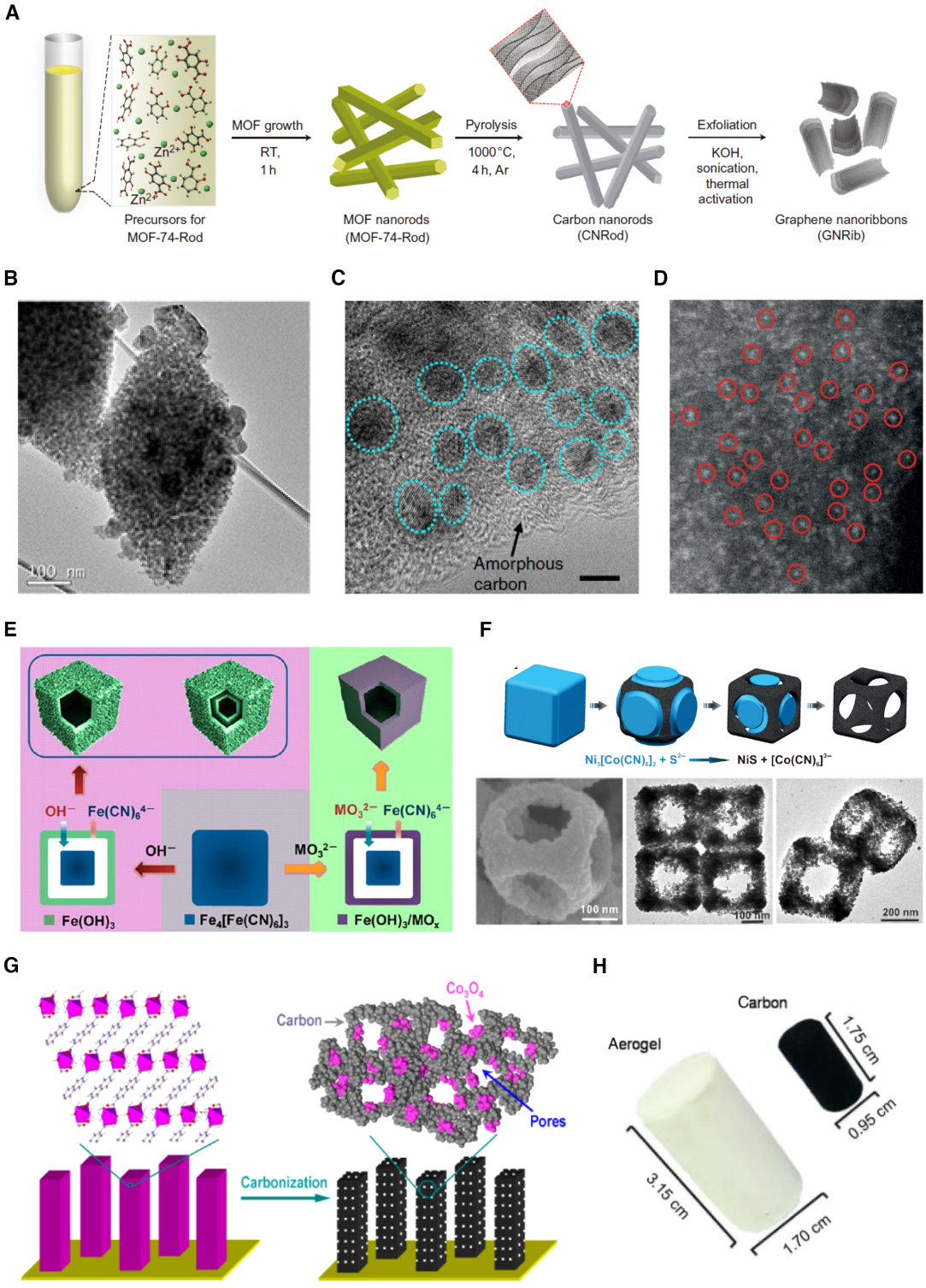

Fig. 6. Morphological and structural control of MOF-derived materials. (**A**) Synthesis of MOF-74-Rod, carbon nanorods, and graphene nanoribbons [(A), adapted with permission from Pachfule *et al.* (*75*)]. RT, room temperature. (**B**) TEM image of mesoporous Fe_2O_3 derived from MIL-88-Fe [(B), adapted with permission from Xu *et al.* (*109*)]. (**C**) High-resolution TEM image of mesoporous MoC_x derived from NENU-5 [(C), adapted with permission from Wu *et al.* (*102*)]. (**D**) High-angle annular dark-field scanning TEM image of single iron atoms (red circles) on N-doped porous carbon [(D), adapted with permission from Chen *et al.* (*104*)]. (**E**) Synthesis of complex hollow structures with multishells (left route) or multicompositions (right route) from Prussian blue [(E), adapted with permission from Zhang *et al.* (*90*)]. (**F**) Schematic of formation of NiS nanoframes from Ni-Co PBA nanocubes (upper) and microscope images of NiS nanoframes (lower) [(F), adapted with permission from Yu *et al.* (*92*)]. (**G**) Fabrication of hybrid Co_3O_4-carbon porous nanowire arrays using Co-based MOF arrays [(G), adapted with permission from Ma *et al.* (*118*)]. (**H**) Photograph of a MOF aerogel monolith and derived carbon monolith [(H), adapted with permission from Xia *et al.* (*121*)].

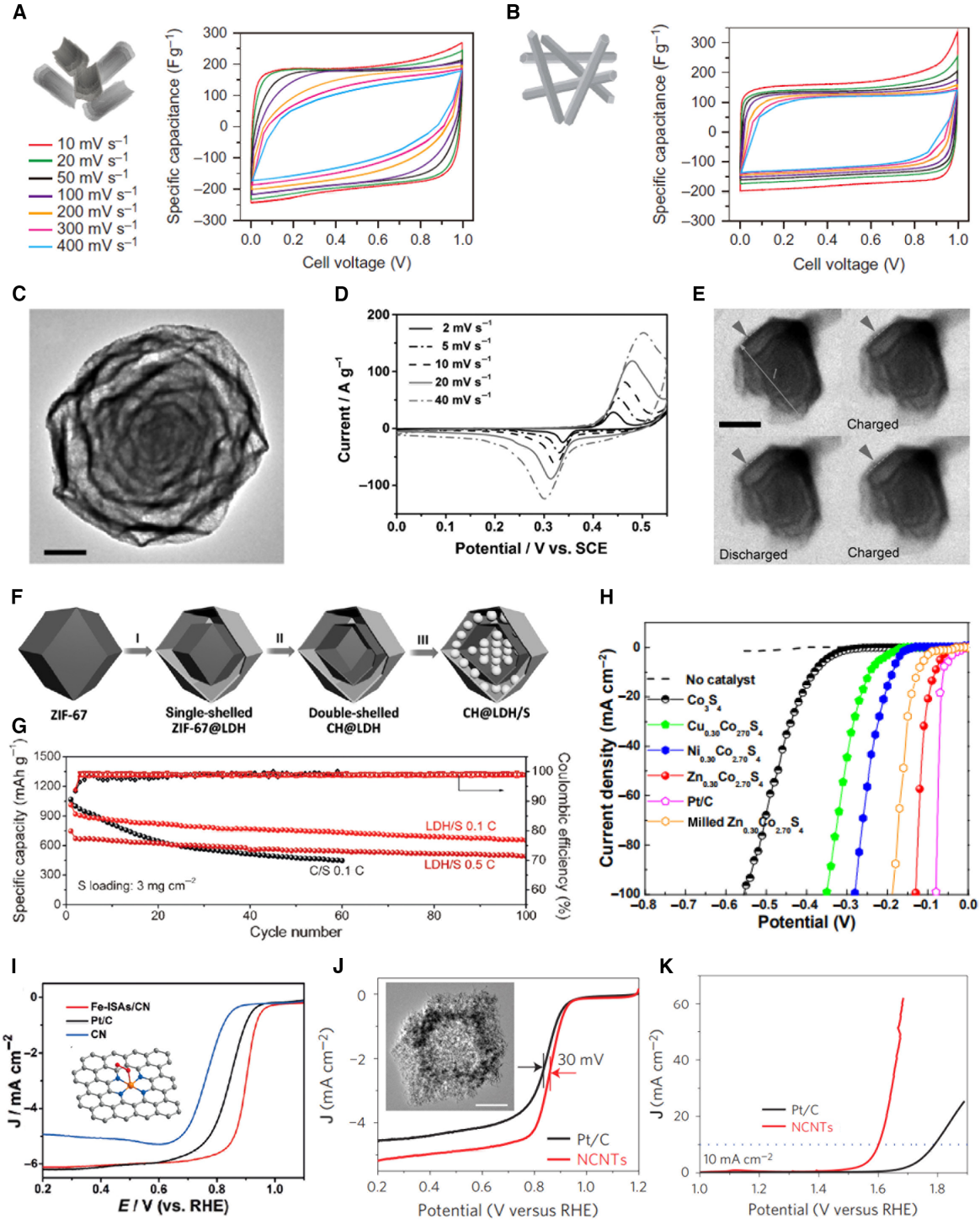

Fig. 7. Functionalities and applications of MOF-derived materials. (**A** and **B**) Carbon nanorods and graphene nanoribbons derived from MOF-74-Rod for electrochemical capacitors: morphology illustrations and cyclic voltammograms (CVs) of (A) carbon nanorods and (B) graphene nanoribbons in 1 M H_2SO_4 electrolyte [(A) and (B), adapted with permission from Pachfule *et al*. (*75*)]. (**C** to **E**) Multishelled Ni-Co oxide hollow particles for charge storage: (C) TEM image and (D) CVs of Ni-Co oxide hollow particles and (E) in situ liquid-cell TEM observation of charge/discharge processes [(C) to (E), adapted with permission from Guan *et al*. (*124*)]. (**F** and **G**) Double-shelled hydroxide hollow particles (CH@LDH) as a sulfur host for Li-S batteries: (F) synthesis of sulfur-loaded double-shelled CH@LDH particles and (G) their cycling performance compared with a conventional mesoporous carbon/sulfur composite [(F) and (G), adapted with permission from Zhang *et al*. (*91*)]. (**H**) Polarization curves of various cobalt-based sulfide particles in 0.5 M H_2SO_4 [(H), adapted with permission from Huang *et al*. (*129*)]. (**I**) Polarization curve of isolated single Fe atoms on N-doped porous carbon (Fe-ISAs/CN) compared with N-doped carbon (CN) and Pt/C in O_2-saturated 0.1 M KOH (inset: scheme of Fe-ISAs/CN) [(I), adapted with permission from Chen *et al*. (*104*)]. (**J** and **K**) Hollow particles of N-doped carbon nanotubes (NCNTs) as a bifunctional catalyst: polarization curves at a rotation rate of 1600 rpm in (J) O_2-saturated 0.1 M KOH and (K) 1 M KOH [(J) and (K), adapted with permission from Xia *et al*. (*82*)].

and modifications, charge carriers with high concentration and mobility can be introduced into MOFs, providing pristine MOFs with high ionic conductivity (*55*).

Most of the studies on ionic conductivity of MOFs have focused on proton conduction (*56*, *57*). Remarkable proton conductivity has been demonstrated in pristine MOFs via the introduction of acidic functional groups on frameworks. For example, a high density of sulfonic acid groups is covalently grafted on the robust framework of Zr-based UiO-66 by a postsynthetic method (Fig. 4A) (*58*). The resulting UiO-66(SO_3H)$_2$ exhibits a superprotonic conductivity of 8.4×10^{-2} S cm^{-1} at 80°C and 90% relative humidity (RH), which is comparable to that of Nafion. MOFs with highly acidic pores can also be obtained by developing framework structures with free acid groups, mostly phosphonate-based MOFs (*59*, *60*). As reported by Taylor *et al.* (*60*), a La-based MOF, PCMOF-5, has uncoordinated phosphonic acid groups from the ligands along the pore channels (Fig. 4B). The highly acidic and hydrated pore channels with potential hydrogen bond pathway enable high proton conductivity above 10^{-3} S cm^{-1} at 60°C and 98% RH; however, the value notably drops at a lower humidity of 90% RH (Fig. 4C). Most proton-conducting MOFs require sufficient hydration because of the roles of water molecules in both Grotthuss and vehicle mechanisms, limiting their applications at temperature above 100°C (*56*).

Another efficient strategy for proton transport in MOFs involves the encapsulation of various protonic molecules, such as triazole, imidazole, histamine, ammonium cations, and Brønsted acids, into the pore channels of MOFs (*61*–*64*). As recently demonstrated by Zhang and coworkers (*65*), imidazole is either physically absorbed by a Fe-based MOF (Im@Fe-MOF) or chemically coordinated to the metal nodes (Im-Fe-MOF) (Fig. 4D). Notably, the proton conductivity of Im-Fe-MOF is about one order of magnitude higher than that of Im@Fe-MOF (Fig. 4E), implying the effect of arrangement of guest molecules. With proper nonvolatile proton carriers and/or Brønsted acid–base pairs in MOFs, facile proton conduction under low humidity or even anhydrous conditions has been demonstrated (*61*, *64*, *66*, *67*). Wei *et al.* (*66*) reported a stable layered MOF with $(Me_2NH_2)^+$ cations periodically aligned in the anionic interlayers, forming strongly hydrogen-bonded chains (Fig. 4F). This MOF delivers a remarkable single-crystal anhydrous conductivity of 1.25×10^{-3} S cm^{-1} at 150°C (Fig. 4G). High proton conductivity at temperature over 100°C has also been demonstrated by loading sulfuric or phosphoric acid in acid-stable MIL-101 (*64*) or by embedding phosphoric acid in defect sites of nonporous coordination polymers (*68*).

Conducting ions other than proton in MOFs is more challenging. Ionic liquid–based lithium electrolytes are infused in the micropores of ZIF-8, a Zn-based MOF, to produce ionic conductors (*69*). Compared with bulk ionic liquid–based electrolytes, incorporating liquid electrolytes in ZIF-8 substantially prohibits the freezing transition and results in improved low-temperature conductivity. Ameloot *et al.* (*70*) and Wiers *et al.* (*71*) demonstrated a strategy to develop lithium-ion conductors by modifying the pore channels of MOFs with lithium alkoxides. Lithium isopropoxide is taken by a Mg-based MOF with 1D channels of ~14 Å (Fig. 4H). After further soaking in a liquid electrolyte ($LiBF_4$ in ethylene carbonate/diethyl carbonate), the dry powder exhibits a remarkable conductivity of 3.1×10^{-4} S cm^{-1} at 300 K, which is much higher than that of MOF treated with only lithium isopropoxide or liquid electrolyte (Fig. 4I). Remarkably, this strategy has been extended to synthesize Mg^{2+} ion conductors by introducing various nucleophilic guest species in the same Mg-based MOF and its analogue with extended pore channels (*72*). These emerging ion conductors are potential alternatives to current polymer/ceramic electrolytes. However, in addition to sufficient ionic conductivity, their chemical/electrochemical stability, mechanical strength, and processability need to be assessed before they could be adapted as electrolytes.

MOF-DERIVED MATERIALS

Compositional control

Along with the attempts to adapt MOF-based materials for energy-related applications, much more efforts have been devoted to converting MOFs or MOF-based composites controllably into inorganic functional materials. These derivatives, collectively termed MOF-derived materials, cover a wide range of chemical compositions, including various carbons, metals/oxides/hydroxides and many other functional materials, and their nanocomposites (*12*–*14*, *18*). Many of these materials have been known to be active for electrochemical applications. Through MOF-derived synthetic approaches, novel compositional and structural features can be created in micrometer/nanometer scales, bringing improved and/or unique properties that are not expected in their conventional counterparts. Generally speaking, there are two basic strategies for controlling the chemical composition of MOF-derived materials (*11*): (i) by tuning the composition of MOF precursors and/or (ii) by manipulating the conversion process. In many cases, these two strategies are adapted simultaneously.

Carbon materials, generally with high porosity, are a good example of inorganic functional materials derived from MOFs (*73*–*76*). Typically, the synthesis involves pyrolysis of MOFs in inert atmosphere followed by an acid-leaching process (this step might be skipped if metal-based species are vaporized), producing porous carbon with high surface area (*73*, *74*). Additional carbon sources (for example, furfuryl alcohol) might be introduced into the pore channels of MOFs to optimize the pore structure of derived carbon (Fig. 5A) (*74*). The graphitic degree of MOF-derived carbon materials is correlated to the metal species in precursors (*77*), whereas heteroatoms such as nitrogen can be simply introduced by linkers (*76*). By constructing core-shell structured particles with two isostructural MOFs (ZIF-8 and ZIF-67), Tang *et al.* (*78*) synthesized hybrid carbon particles with an N-doped core and a highly graphitic shell (Fig. 5B). This work demonstrates the simultaneous formation of graphitic carbon catalytically assisted by transition metals and N-doping from N-containing imidazole linkers.

Typically, pyrolysis of MOFs in air produces corresponding metal oxides (*79*–*81*). Nanocomposites of metal-containing materials and carbon can be produced by pyrolysis of MOFs in a nonoxidative atmosphere without acid leaching. The inorganic materials could be metals, metal oxides, or metal carbides, depending on the type of metal and synthetic conditions (*82*–*85*). Because of the homogeneous and localized reactions between metal nodes and organic linkers in the nanometer scale, the derived materials normally exist as composites of metal-containing nanoparticles or even atoms/clusters and carbonaceous components (*86*–*89*). For example, a one-step controlled pyrolysis of IRMOF-1 (also known as MOF-5) produces well-dispersed carbon-coated ZnO quantum dots of ~3.5 nm in size embedded in an amorphous carbon matrix (Fig. 5C) (*86*). More recently, a novel nanocomposite of single-metal atoms anchored on N-doped carbon has been successfully synthesized from a Zn-Co MOF by taking advantage of the N-coordinated metal centers in the precursor (*87*).

Other than metal oxides, diverse functional materials can be derived from MOFs by reacting MOFs with secondary reactants in the gas or liquid phase. This versatile strategy leads to easy synthesis of hydroxides (*90*, *91*), sulfides (*92*–*94*), selenides (*95*), phosphides (*96*, *97*), and

phosphates (*98*) and their nanocomposites. As demonstrated by Yu and co-workers (*96*), starting with a Ni-based Prussian blue analogue (NiNi-PBA), $Ni(OH)_2$, NiO, and nickel phosphide (Ni-P) have been successfully synthesized (Fig. 5, D and E) via reaction with NaOH solution, calcination in air, and annealing with NaH_2PO_2, respectively. Compared with conventional inorganic precursors, MOFs allow facile transformations to different functional materials in a well-controlled manner.

Nevertheless, it is sometimes difficult to tune the composition of MOF precursors, especially the metal centers, to produce designed functional materials (*99*). Postsynthetic modifications or certain families of MOFs/open frameworks might allow modification of metal centers to some degree (*100*, *101*). A feasible and versatile strategy is to introduce metal-containing guests in the pore channels of MOFs, as demonstrated by the successful synthesis of early transition metal carbides (*102*) and oxides (*103*). Specifically, a hybrid MOF (NENU-5), consisting of a well-studied HKUST-1 host and Mo-based polyoxometalate (POM) guest species residing in the pores, is subjected to pyrolysis in inert gas followed by an etching process, resulting in the formation of mesoporous molybdenum carbide (MoC_x) octahedral particles (Fig. 5F) (*102*). Under optimized pyrolysis conditions, similar hybrid MOF particles supported on graphene oxide sheets are successfully converted to MoO_2-based nanocomposites (Fig. 5G) (*103*). Other metal salts or complexes could also be loaded into MOFs to introduce desirable constituents in the derived materials (*104*–*106*). In addition, secondary components as preformed particles can be incorporated into MOF particles, forming two-phase composites (*107*). A noteworthy example is a MOF-in-MOF composite by assembling two different MOFs, MIL-88B and ZIF-8 (Fig. 5, H and I) (*84*). Direct pyrolysis of the MOF composite produces Fe_3C nanoparticles embedded in N-doped carbon nanotubes (Fe_3C@N-CNTs), where the iron and nitrogen moieties come from MIL-88B and ZIF-8, respectively.

Morphological and structural control

Creating functional materials with unique morphologies and structures in the micrometer/nanometer scale has been a major motivation for developing MOF-derived synthetic methods (*11*, *13*, *18*, *108*). MOFs generally serve as both precursors and templates for derived materials, which are excellent examples of self-templated synthesis. The morphology and structure of MOF-derived materials can be effectively engineered by means of synthesizing MOF-based precursors with nanoscale morphological features, for example, (sub-)micrometer-sized particles, hollow/frame-like structures, and MOF-containing nanocomposites (*11*). Moreover, compositional control of MOF-derived materials during the conversion process is always accompanied by the formation of unusual microstructures/nanostructures. Therefore, the MOF-based precursor and the conversion method together determine the morphology/structure of the derived materials. There are two notable features for these MOF-derived strategies. First, high porosity of MOFs and loss of certain organic moieties during the conversion process lead to abundant cavities in MOF-derived materials, typically forming porous and/or hollow structures. Second, the moderate thermodynamic stability of MOFs allows the conversion into inorganic functional materials in a controllable manner, which enables the manipulation and tuning of derived structures.

A porous structure is the most basic structure that one can expect from MOF-derived materials. Carbonaceous materials synthesized by pyrolysis of MOF-based precursors typically exhibit nanoporous feature and high surface area (*73*, *74*, *76*, *78*). For example, microporous carbon derived from ZIF-8 has shown a very high Brunauer-Emmett-Teller surface area over 3400 $m^2\ g^{-1}$ under optimized conditions (*74*), which is significantly higher than that of conventional porous carbon materials. Low-dimensional carbon materials, such as carbon nanotubes or graphene, have been reported in the presence of catalytically active metals (*82*, *105*). Recently, an unusual method has been developed to synthesize 1D carbon nanorods and 2D graphene nanoribbons (*75*). Here, direct pyrolysis of a rod-shaped MOF precursor (MOF-74-Rod) produces carbon nanorods, which are further exfoliated to obtain graphene nanoribbons (Fig. 6A).

Other than carbon, porous metal oxides can be prepared by pyrolysis of MOFs in air. However, it is more challenging to maintain an integrated structure and large surface area because of the complete loss of organic components and unavoidable coalescence of nanoparticles. For example, a two-step pyrolysis method has been found to be indispensable for synthesizing spindle-like mesoporous Fe_2O_3 particles (Fig. 6B) (*109*). Alternatively, porous structures of metal-based inorganic materials are usually constructed with the assistance of carbonaceous components, such as metal-based moieties supported on the porous carbon matrix or carbon-coated porous metal–based compounds (*86*, *87*, *102*, *104*, *110*). The presence of carbon matrix would effectively prevent the excessive growth and agglomeration of metal-containing moieties, as well as the diminishment of the surface area during high-temperature synthesis, as exemplified by the synthesis of mesoporous MoC_x polyhedral particles via a confined pyrolysis strategy (Fig. 6C) (*102*). More recently, isolated single metal atoms have been successfully stabilized and anchored on an N-doped porous carbon (Fig. 6D) (*104*).

In view of the large volume loss during the conversion process, MOFs are especially suitable as precursors for the fabrication of hollow and frame-like structures (*11*). The formation of hollow structures could be achieved via selective etching of solid MOF particles (*111*). More commonly, hollow cavities appear during the conversion process, for example, through outward diffusion in solution-based reactions or heterogeneous contraction during thermal decomposition (*11*). By precisely manipulating the reactions, complex hollow structures, such as multishells, hierarchical shells, multiple compositions, and anisotropic structures, have been fabricated using MOF-based precursors (*80*, *90*–*93*, *112*). For example, starting with Prussian blue cubic particles, multishelled hollow microcubes composed of $Fe(OH)_3$ nanosheets and multicompositional hollow microcubes of two metal oxides/hydroxides have been prepared (Fig. 6E) (*90*). By reacting Ni-Co PBA nanocubes with S^{2-} ions in solution, the ion exchange reaction preferentially occurs at the edge of nanocubes with high curvature and probably higher reactivity (Fig. 6F) (*92*). This anisotropic reaction on PBA nanocubes eventually creates an unusual frame-like structure.

Additional functionalities and/or morphological features could be introduced by assembling MOFs with or depositing MOFs on preformed materials, such as mesoporous carbon, graphene, and polymer fibers (*113*–*116*). Functional materials derived from these composite precursors generally exhibit hierarchical or 3D architectures. Although most MOF-derived materials are in powder form, constructing 3D bulk materials such as films and monoliths has gained increasing interests. Freestanding films could be fabricated by depositing MOFs on proper substrates, such as porous graphene films, carbon cloths, and metal foils (*117*–*120*). As reported by Ma *et al.* (*118*), hybrid porous nanowire arrays of Co_3O_4 nanoparticles supported on carbon have been successfully synthesized by pyrolysis of arrays of MOF nanowires on Cu foil (Fig. 6G). Another good example of MOF-derived bulk materials is the synthesis of a porous carbon monolith from a MOF aerogel (Fig. 6H) (*121*). In these MOF-derived 3D bulk architectures, the structural features

in the micrometer/nanometer scale (for example, low-dimensional morphology and nanoporosity) are organized in the macroscopic scale, which might benefit their uses as active components in electrochemical devices.

Functionalities and applications

Microstructures/nanostructures have been well known to effectively modulate the physical/chemical properties of inorganic functional materials. As discussed in previous sections, MOF-derived synthesis strategies enable tunable compositions and designable structures of materials, which might boost their electrochemical performance. Specifically, by tuning the chemical compositions and/or incorporating multiple components, the inherent electrochemical activity of MOF-derived materials could be modulated and enhanced. Meanwhile, the high porosity and large surface area of MOF-derived materials provide large electrochemically active surface, facile charge/mass transport, and efficient accommodation of strain during electrochemical processes (*11*–*13*, *15*). When applied to electrochemical energy–related applications, these compositional and structural features bring substantial advantages to MOF-derived materials compared with their counterparts synthesized by conventional methods.

For electrochemical capacitors, the double-layer capacitance in carbon-based materials is highly related to the pore structure and surface area. Nanoporous carbon materials derived from MOFs usually have a large surface area and uniform micropores, which are attractive features for double-layer charge storage (*3*). The charge storage properties can be further improved by modulating the pore structure and/or morphology (*75*, *122*). The recently reported low-dimensional porous carbon materials derived from MOF-74-Rod exhibit high double-layer capacitances (*75*). In particular, the 2D carbon nanoribbons deliver a remarkable specific capacitance of 193 F g^{-1} at 10 mV s^{-1} in a symmetric two-electrode cell with a voltage window of 1.0 V (Fig. 7A), which is superior to the carbon nanorods (Fig. 7B). Moreover, doping of heteroatoms (for example, nitrogen) might introduce Faradaic charge storage and/or improve electronic conductivity, whereas a higher graphitic degree might lead to increased electronic conductivity but reduced surface area (*78*). All these features can be modulated through tuning the precursors, synthetic conditions, posttreatment, and so on, making MOF-derived carbon materials promising candidates for electrochemical capacitors (*17*).

MOF-derived electrode materials for batteries usually have two major advantages. First, high porosity and large surface area promote the ion transport and insertion within the porous structure, leading to higher reversible capacity and improved kinetics. Second, the abundant cavities sometimes with carbonaceous components accommodate mechanical strain during repeated ion insertion/de-insertion, leading to prolonged cycle life. These merits not only help to develop advanced electrode materials for conventional LIBs but also work for battery-type electrodes in hybrid supercapacitors (HSCs). An HSC combines a carbon-based capacitor-type electrode and a battery-type electrode, potentially delivering both high energy and power densities (*123*). Fast kinetics and long life span are required in the battery-type electrode, which could be realized by constructing hollow structures from MOFs. Guan *et al.* (*124*, *125*) recently demonstrated a general coordination polymer–derived approach for multishelled mixed metal oxides (Fig. 7C) and sulfides. These complex hollow particles with thin Ni-Co oxide shells give rise to fast Faradaic redox processes despite their battery-type behavior (Fig. 7D). Minimal volume change is observed during charge/discharge by in situ liquid-cell TEM (Fig. 7E).

The tunable porous structure and composition also allow the designed synthesis of advanced host materials for sulfur in Li-S batteries. MOF-derived carbon hosts with various porous structures have been actively explored to encapsulate sulfur (*121*, *126*, *127*). In particular, micropores have been found to induce some strong confinement effect with guest species, thus altering the electrochemical behavior of the carbon-sulfur composite electrodes (*127*). To increase the loading amount of sulfur and strengthen the encapsulation of polysulfides, hollow structures containing polar metal compounds would be promising hosts by providing both physical barriers and chemical sorption to active species (*128*). As a proof of concept, Zhang *et al.* (*91*) designed and synthesized double-shelled hollow structures of cobalt hydroxide and layered double hydroxides (CH@LDH) starting from ZIF-67 particles (Fig. 7F). After loading of 75 weight % of sulfur in the hollow structures, the composite electrode delivers much improved cycling stability compared with a conventional mesoporous carbon/sulfur material (Fig. 7G).

MOF-derived materials have also been found attractive as electrocatalysts. Tuning the chemical composition would significantly affect the inherent catalytic activity. For example, Huang *et al.* (*129*) reported a general MOF-derived approach toward hollow polyhedral particles of Co-based bimetallic sulfides. By modulating the chemical composition, $Zn_{0.3}Co_{2.7}S_4$ hollow particles exhibit the best HER activity among the investigated samples (Fig. 7H). To further increase the exposure of active sites, the size of metal-based active components has been reduced to ultrafine nanoparticles or even single atoms supported on porous carbon matrix (*87*, *102*, *110*). A noteworthy example is a family of noble metal–free ORR electrocatalysts based on nanocrystallites or even atoms of transition metals loaded on N-doped carbon materials, for which MOFs with imidazole-type ligands have been widely used as precursors (*47*, *104*, *130*). The isolated Fe atoms anchored on N-doped carbon support represent the upper limit of atomic efficiency for catalysis (*104*), with remarkable ORR activity exceeding that of Pt/C catalyst in alkaline electrolytes (Fig. 7I).

MOF-derived electrocatalysts have been extensively reported in the past few years and have been applied to most of the important energy conversion reactions, including HER and OER for water splitting, ORR for fuel cells, and even CO_2 reduction (*8*, *15*). Many electrocatalysts also exhibit multiple functionalities by catalyzing more than one reaction (*83*, *89*). Of particular interest is the development of bifunctional electrocatalysts for OER and ORR, which are important for the operation of cathode in rechargeable metal-air batteries. Hollow particles composed of NCNTs reported by Xia *et al.* (*82*) represent an excellent example. In alkaline electrolyte, this NCNT catalyst derived from ZIF-67 manifests better ORR activity and durability than a commercial Pt/C catalyst (Fig. 7J); similar superiority is observed for the OER activity (Fig. 7K). The remarkable electrocatalytic activity and stability would be related to the hierarchical hollow structure with a large surface area and the highly active and robust graphitic NCNTs.

CONCLUSIONS

In retrospect, new technologies and/or breakthrough advances in existing ones usually come with the development of new materials. Perhaps we are now witnessing a revolution brought by MOFs to the field of renewable energy technologies. MOF-related materials have been demonstrated as potential candidates for essential components in electrochemical energy storage and conversion devices, such as electrode materials, electrocatalysts, and electrolytes. The promising physical/physicochemical properties expected in these electrochemically active

materials, including charge transport/storage properties and electrocatalytic activities, can be realized and modulated in both MOF-based and MOF-derived materials by proper compositional and structural engineering.

The research of MOF-based materials for electrochemical energy storage and conversion is still at its infancy stage. Despite a few particular groups of materials, that is, Prussian blue and its analogues for ion storage and proton-conducting MOFs, reports on MOF-based electrode materials, electrocatalysts, and electrolytes are still limited. It has been known that both metal and organic moieties can contribute to the electrochemical activity. Additional functionalities such as ion conductivity can be realized by forming nanocomposites. The open-framework structures, in principle, maximize the utilization of atoms/molecules, and they are also essential for charge/mass storage and transport. However, the insulating nature of most existing MOFs hampers their adaptation as electrode materials and electrocatalysts. The emergence of new MOFs with high electronic conductivity represents a feasible solution. Meanwhile, MOF-based electrolytes for ions other than proton are important for batteries but are rarely reported to date. In future studies, theoretical prediction based on computational modeling might significantly aid the discovery of new MOFs for electrochemical applications. In addition, the stability of MOF-based materials during ion insertion and operation in highly corrosive electrolytes remains another critical issue.

MOF-derived materials for electrochemical applications have been under intensive investigation in the past few years. MOFs serve as an important platform for the development of advanced inorganic functional materials. New features and properties have been brought to many known inorganic materials derived from MOF-based precursors. More specifically, the MOF-derived strategy is unique and efficient for porous and/or hollow microstructures/nanostructures and nanocomposites with strongly coupled metal-based moieties and carbon. The self-templated feature of many MOF-derived approaches simplifies the synthetic procedures, possibly allowing large-scale production. Nevertheless, most reports are based on individual systems; universal and general synthetic approaches are highly desirable but still limited. From a practical point of view, starting with low-cost and easily synthesized MOFs would be more appealing. Finally, an in-depth understanding of the formation processes of MOF-derived materials and their composition/structure-dependent properties is still lacking, where computational and theoretical approaches would play important roles in future studies.

Overall, the development of MOF-related materials for electrochemical energy storage and conversion has been an exciting interdisciplinary area, where opportunities and challenges coexist. One might expect rapid development of MOF-related functional materials from materials design and synthesis, evaluation of properties, fundamental understanding, and eventually to practical applications. In addition to fundamental research, low-cost and industrial production of MOFs has already been successfully demonstrated, for example, the Basolite series developed by BASF SE. In view of the continuous progress on scale-up synthesis of MOFs (*131*), the widespread use of MOF-related materials for industrial and domestic applications is highly feasible. With continued research efforts in the related fields, it is likely for us to witness a revolution of renewable energy utilization in the near future.

REFERENCES AND NOTES

1. B. Dunn, H. Kamath, J.-M. Tarascon, Electrical energy storage for the grid: A battery of choices. *Science* **334**, 928–935 (2011).
2. Z. W. Seh, J. Kibsgaard, C. F. Dickens, I. Chorkendorff, J. K. Nørskov, T. F. Jaramillo, Combining theory and experiment in electrocatalysis: Insights into materials design. *Science* **355**, eaad4998 (2017).
3. M. Winter, R. J. Brodd, What are batteries, fuel cells, and supercapacitors? *Chem. Rev.* **104**, 4245–4270 (2004).
4. H. Furukawa, K. E. Cordova, M. O'Keeffe, O. M. Yaghi, The chemistry and applications of metal-organic frameworks. *Science* **341**, 1230444 (2013).
5. H.-C. Zhou, J. R. Long, O. M. Yaghi, Introduction to metal–organic frameworks. *Chem. Rev.* **112**, 673–674 (2012).
6. J. Liang, Z. Liang, R. Zou, Y. Zhao, Heterogeneous catalysis in zeolites, mesoporous silica, and metal–organic frameworks. *Adv. Mater.* **29**, 1701139 (2017).
7. H. Zhang, J. Nai, L. Yu, X. W. Lou, Metal-organic-framework-based materials as platforms for renewable energy and environmental applications. *Joule* **1**, 77–107 (2017).
8. A. Mahmood, W. Guo, H. Tabassum, R. Zou, Metal-organic framework-based nanomaterials for electrocatalysis. *Adv. Energy Mater.* **6**, 1600423 (2016).
9. H. Wang, Q.-L. Zhu, R. Zou, Q. Xu, Metal-organic frameworks for energy applications. *Chem* **2**, 52–80 (2017).
10. L. Wang, Y. Han, X. Feng, J. Zhou, P. Qi, B. Wang, Metal–organic frameworks for energy storage: Batteries and supercapacitors. *Coord. Chem. Rev.* **307**, 361–381 (2016).
11. B. Y. Guan, X. Y. Yu, H. B. Wu, X. W. Lou, Complex nanostructures from materials based on metal–organic frameworks for electrochemical energy storage and conversion. *Adv. Mater.* **2017**, 1703614 (2017).
12. J.-K. Sun, Q. Xu, Functional materials derived from open framework templates/precursors: Synthesis and applications. *Energy Environ. Sci.* **7**, 2071–2100 (2014).
13. X. Cao, C. Tan, M. Sindoro, H. Zhang, Hybrid micro-/nano-structures derived from metal–organic frameworks: Preparation and applications in energy storage and conversion. *Chem. Soc. Rev.* **46**, 2660–2677 (2017).
14. Y. V. Kaneti, J. Tang, R. R. Salunkhe, X. Jiang, A. Yu, K. C.-W. Wu, Y. Yamauchi, Nanoarchitectured design of porous materials and nanocomposites from metal-organic frameworks. *Adv. Mater.* **29**, 1604898 (2017).
15. J. Liu, D. Zhu, C. Guo, A. Vasileff, S.-Z. Qiao, Design strategies toward advanced MOF-derived electrocatalysts for energy-conversion reactions. *Adv. Energy Mater.* **2017**, 1700518 (2017).
16. W. Wang, X. Xu, W. Zhou, Z. Shao, Recent progress in metal-organic frameworks for applications in electrocatalytic and photocatalytic water splitting. *Adv. Sci.* **4**, 1600371 (2017).
17. Z. Xie, W. Xu, X. Cui, Y. Wang, Recent progress in metal–organic frameworks and their derived nanostructures for energy and environmental applications. *ChemSusChem* **10**, 1645–1663 (2017).
18. W. Xia, A. Mahmood, R. Zou, Q. Xu, Metal–organic frameworks and their derived nanostructures for electrochemical energy storage and conversion. *Energy Environ. Sci.* **8**, 1837–1866 (2015).
19. S. Zheng, X. Li, B. Yan, Q. Hu, Y. Xu, X. Xiao, H. Xue, H. Pang, Transition-metal (Fe, Co, Ni) based metal-organic frameworks for electrochemical energy storage. *Adv. Energy Mater.* **7**, 1602733 (2017).
20. P. Simon, Y. Gogotsi, B. Dunn, Where do batteries end and supercapacitors begin? *Science* **343**, 1210–1211 (2014).
21. G. Férey, F. Millange, M. Morcrette, C. Serre, M.-L. Doublet, J.-M. Grenèche, J.-M. Tarascon, Mixed-valence Li/Fe-based metal–organic frameworks with both reversible redox and sorption properties. *Angew. Chem. Int. Ed.* **46**, 3259–3263 (2007).
22. J. Shin, M. Kim, J. Cirera, S. Chen, G. J. Halder, T. A. Yersak, F. Paesani, S. M. Cohen, Y. S. Meng, MIL-101(Fe) as a lithium-ion battery electrode material: A relaxation and intercalation mechanism during lithium insertion. *J. Mater. Chem. A* **3**, 4738–4744 (2015).
23. K. Saravanan, M. Nagarathinam, P. Balaya, J. J. Vittal, Lithium storage in a metal organic framework with diamondoid topology – A case study on metal formates. *J. Mater. Chem.* **20**, 8329–8335 (2010).
24. Y. Jin, C. Zhao, Z. Sun, Y. Lin, L. Chen, D. Wang, C. Shen, Facile synthesis of Fe-MOF/RGO and its application as a high performance anode in lithium-ion batteries. *RSC Adv.* **6**, 30763–30768 (2016).
25. Z. Zhang, H. Yoshikawa, K. Awaga, Monitoring the solid-state electrochemistry of Cu(2,7-AQDC) (AQDC = anthraquinone dicarboxylate) in a lithium battery: Coexistence of metal and ligand redox activities in a metal–organic framework. *J. Am. Chem. Soc.* **136**, 16112–16115 (2014).
26. C. Fang, Y. Huang, L. Yuan, Y. Liu, W. Chen, Y. Huang, K. Chen, J. Han, Q. Liu, Y. Huang, A metal–organic compound as cathode material with superhigh capacity achieved by reversible cationic and anionic redox chemistry for high-energy sodium-ion batteries. *Angew. Chem. Int. Ed.* **56**, 6793–6797 (2017).
27. H.-W. Lee, R. Y. Wang, M. Pasta, S. Woo Lee, N. Liu, Y. Cui, Manganese hexacyanomanganate open framework as a high-capacity positive electrode material for sodium-ion batteries. *Nat. Commun.* **5**, 5280 (2014).

28. Y. You, X.-L. Wu, Y.-X. Yin, Y.-G. Guo, High-quality Prussian blue crystals as superior cathode materials for room-temperature sodium-ion batteries. *Energy Environ. Sci.* **7**, 1643–1647 (2014).
29. L. Xue, Y. Li, H. Gao, W. Zhou, X. Lü, W. Kaveevivitchai, A. Manthiram, J. B. Goodenough, Low-cost high-energy potassium cathode. *J. Am. Chem. Soc.* **139**, 2164–2167 (2017).
30. P. Nie, L. Shen, H. Luo, B. Ding, G. Xu, J. Wang, X. Zhang, Prussian blue analogues: A new class of anode materials for lithium ion batteries. *J. Mater. Chem. A* **2**, 5852–5857 (2014).
31. Y. You, H.-R. Yao, S. Xin, Y.-X. Yin, T.-T. Zuo, C.-P. Yang, Y.-G. Guo, Y. Cui, L.-J. Wan, J. B. Goodenough, Subzero-temperature cathode for a sodium-ion battery. *Adv. Mater.* **28**, 7243–7248 (2016).
32. R. Y. Wang, B. Shyam, K. H. Stone, J. N. Weker, M. Pasta, H.-W. Lee, M. F. Toney, Y. Cui, Reversible multivalent (monovalent, divalent, trivalent) ion insertion in open framework materials. *Adv. Energy Mater.* **5**, 1401869 (2015).
33. M. L. Aubrey, J. R. Long, A dual–ion battery cathode via oxidative insertion of anions in a metal–organic framework. *J. Am. Chem. Soc.* **137**, 13594–13602 (2015).
34. K. M. Choi, H. M. Jeong, J. H. Park, Y. B. Zhang, J. K. Kang, O. M. Yaghi, Supercapacitors of nanocrystalline metal–organic frameworks. *ACS Nano* **8**, 7451–7457 (2014).
35. L. Sun, M. G. Campbell, M. Dincă, Electrically conductive porous metal–organic frameworks. *Angew. Chem. Int. Ed.* **55**, 3566–3579 (2016).
36. D. Sheberla, J. C. Bachman, J. S. Elias, C.-J. Sun, Y. Shao-Horn, M. Dincă, Conductive MOF electrodes for stable supercapacitors with high areal capacitance. *Nat. Mater.* **16**, 220–224 (2017).
37. D. Wu, Z. Guo, X. Yin, Q. Pang, B. Tu, L. Zhang, Y.-G. Wang, Q. Li, Metal–organic frameworks as cathode materials for Li–O_2 batteries. *Adv. Mater.* **26**, 3258–3262 (2014).
38. J. Zheng, J. Tian, D. Wu, M. Gu, W. Xu, C. Wang, F. Gao, M. H. Engelhard, J.-G. Zhang, J. Liu, J. Xiao, Lewis acid–base interactions between polysulfides and metal organic framework in lithium sulfur batteries. *Nano Lett.* **14**, 2345–2352 (2014).
39. H. Park, D. J. Siegel, Tuning the adsorption of polysulfides in lithium–sulfur batteries with metal–organic frameworks. *Chem. Mater.* **29**, 4932–4939 (2017).
40. J. Zhou, R. Li, X. Fan, Y. Chen, R. Han, W. Li, J. Zheng, B. Wang, X. Li, Rational design of a metal–organic framework host for sulfur storage in fast, long-cycle Li–S batteries. *Energy Environ. Sci.* **7**, 2715–2724 (2014).
41. Y. P. Zhu, C. Guo, Y. Zheng, S.-Z. Qiao, Surface and interface engineering of noble-metal-free electrocatalysts for efficient energy conversion processes. *Acc. Chem. Res.* **50**, 915–923 (2017).
42. P. M. Usov, B. Huffman, C. C. Epley, M. C. Kessinger, J. Zhu, W. A. Maza, A. J. Morris, Study of electrocatalytic properties of metal–organic framework PCN-223 for the oxygen reduction reaction. *ACS Appl. Mater. Interfaces* **9**, 33539–33543 (2017).
43. N. Kornienko, Y. Zhao, C. S. Kley, C. Zhu, D. Kim, S. Lin, C. J. Chang, O. M. Yaghi, P. Yang, Metal–organic frameworks for electrocatalytic reduction of carbon dioxide. *J. Am. Chem. Soc.* **137**, 14129–14135 (2015).
44. A. J. Clough, J. W. Yoo, M. H. Mecklenburg, S. C. Marinescu, Two-dimensional metal–organic surfaces for efficient hydrogen evolution from water. *J. Am. Chem. Soc.* **137**, 118–121 (2015).
45. E. M. Miner, T. Fukushima, D. Sheberla, L. Sun, Y. Surendranath, M. Dincă, Electrochemical oxygen reduction catalysed by Ni_3(hexaiminotriphenylene)$_2$. *Nat. Commun.* **7**, 10942 (2016).
46. S. Zhao, Y. Wang, J. Dong, C.-T. He, H. Yin, P. An, K. Zhao, X. Zhang, C. Gao, L. Zhang, J. Lv, J. Wang, J. Zhang, A. M. Khattak, N. A. Khan, Z. Wei, J. Zhang, S. Liu, H. Zhao, Z. Tang, Ultrathin metal–organic framework nanosheets for electrocatalytic oxygen evolution. *Nat. Energy* **1**, 16184 (2016).
47. A. Zitolo, V. Goellner, V. Armel, M.-T. Sougrati, T. Mineva, L. Stievano, E. Fonda, F. Jaouen, Identification of catalytic sites for oxygen reduction in iron- and nitrogen-doped graphene materials. *Nat. Mater.* **14**, 937–942 (2015).
48. C. A. Downes, S. C. Marinescu, Efficient electrochemical and photoelectrochemical H_2 production from water by a cobalt dithiolene one-dimensional metal–organic surface. *J. Am. Chem. Soc.* **137**, 13740–13743 (2015).
49. A. J. Clough, J. M. Skelton, C. A. Downes, A. A. de la Rosa, J. W. Yoo, A. Walsh, B. C. Melot, S. C. Marinescu, Metallic conductivity in a two-dimensional cobalt dithiolene metal–organic framework. *J. Am. Chem. Soc.* **139**, 10863–10867 (2017).
50. J.-Q. Shen, P.-Q. Liao, D.-D. Zhou, C.-T. He, J.-X. Wu, W.-X. Zhang, J.-P. Zhang, X.-M. Chen, Modular and stepwise synthesis of a hybrid metal–organic framework for efficient electrocatalytic oxygen evolution. *J. Am. Chem. Soc.* **139**, 1778–1781 (2017).
51. P. Manna, J. Debgupta, S. Bose, S. K. Das, A mononuclear Co^{II} coordination complex locked in a confined space and acting as an electrochemical water-oxidation catalyst: A "ship-in-a-bottle" approach. *Angew. Chem. Int. Ed.* **55**, 2425–2430 (2016).
52. A. J. Howarth, Y. Liu, P. Li, Z. Li, T. C. Wang, J. T. Hupp, O. K. Farha, Chemical, thermal and mechanical stabilities of metal–organic frameworks. *Nat. Rev. Mater.* **1**, 15018 (2016).
53. X.-F. Lu, P.-Q. Liao, J.-W. Wang, J.-X. Wu, X.-W. Chen, C.-T. He, J.-P. Zhang, G.-R. Li, X.-M. Chen, An alkaline-stable, metal hydroxide mimicking metal–organic framework for efficient electrocatalytic oxygen evolution. *J. Am. Chem. Soc.* **138**, 8336–8339 (2016).
54. I. Hod, P. Deria, W. Bury, J. E. Mondloch, C.-W. Kung, M. So, M. D. Sampson, A. W. Peters, C. P. Kubiak, O. K. Farha, J. T. Hupp, A porous proton-relaying metal-organic framework material that accelerates electrochemical hydrogen evolution. *Nat. Commun.* **6**, 8304 (2015).
55. S. Horike, D. Umeyama, S. Kitagawa, Ion conductivity and transport by porous coordination polymers and metal–organic frameworks. *Acc. Chem. Res.* **46**, 2376–2384 (2013).
56. P. Ramaswamy, N. E. Wong, G. K. H. Shimizu, MOFs as proton conductors—Challenges and opportunities. *Chem. Soc. Rev.* **43**, 5913–5932 (2014).
57. A.-L. Li, Q. Gao, J. Xu, X.-H. Bu, Proton-conductive metal-organic frameworks: Recent advances and perspectives. *Coord. Chem. Rev.* **344**, 54–82 (2017).
58. W. J. Phang, H. Jo, W. R. Lee, J. H. Song, K. Yoo, B. Kim, C. S. Hong, Superprotonic conductivity of a UiO-66 framework functionalized with sulfonic acid groups by facile postsynthetic oxidation. *Angew. Chem. Int. Ed.* **54**, 5142–5146 (2015).
59. S. Pili, S. P. Argent, C. G. Morris, P. Rought, V. García-Sakai, I. P. Silverwood, T. L. Easun, M. Li, M. R. Warren, C. A. Murray, C. C. Tang, S. Yang, M. Schröder, Proton conduction in a phosphonate-based metal–organic framework mediated by intrinsic "free diffusion inside a sphere". *J. Am. Chem. Soc.* **138**, 6352–6355 (2016).
60. J. M. Taylor, K. W. Dawson, G. K. H. Shimizu, A water-stable metal–organic framework with highly acidic pores for proton-conducting applications. *J. Am. Chem. Soc.* **135**, 1193–1196 (2013).
61. J. A. Hurd, R. Vaidhyanathan, V. Thangadurai, C. I. Ratcliffe, I. L. Moudrakovski, G. K. H. Shimizu, Anhydrous proton conduction at 150°C in a crystalline metal–organic framework. *Nat. Chem.* **1**, 705–710 (2009).
62. S. S. Nagarkar, S. M. Unni, A. Sharma, S. Kurungot, S. K. Ghosh, Two-in-one: Inherent anhydrous and water-assisted high proton conduction in a 3D metal–organic framework. *Angew. Chem. Int. Ed.* **53**, 2638–2642 (2014).
63. D. Umeyama, S. Horike, M. Inukai, Y. Hijikata, S. Kitagawa, Confinement of mobile histamine in coordination nanochannels for fast proton transfer. *Angew. Chem. Int. Ed.* **50**, 11706–11709 (2011).
64. V. G. Ponomareva, K. A. Kovalenko, A. P. Chupakhin, D. N. Dybtsev, E. S. Shutova, V. P. Fedin, Imparting high proton conductivity to a metal–organic framework material by controlled acid impregnation. *J. Am. Chem. Soc.* **134**, 15640–15643 (2012).
65. F.-M. Zhang, L.-Z. Dong, J.-S. Qin, W. Guan, J. Liu, S.-L. Li, M. Lu, Y.-Q. Lan, Z.-M. Su, H.-C. Zhou, Effect of imidazole arrangements on proton-conductivity in metal–organic frameworks. *J. Am. Chem. Soc.* **139**, 6183–6189 (2017).
66. Y.-S. Wei, X.-P. Hu, Z. Han, X.-Y. Dong, S.-Q. Zang, T. C. W. Mak, Unique proton dynamics in an efficient MOF-based proton conductor. *J. Am. Chem. Soc.* **139**, 3505–3512 (2017).
67. B. Joarder, J.-B. Lin, Z. Romero, G. K. H. Shimizu, Single crystal proton conduction study of a metal organic framework of modest water stability. *J. Am. Chem. Soc.* **139**, 7176–7179 (2017).
68. M. Inukai, S. Horike, T. Itakura, R. Shinozaki, N. Ogiwara, D. Umeyama, S. Nagarkar, Y. Nishiyama, M. Malon, A. Hayashi, T. Ohhara, R. Kiyanagi, S. Kitagawa, Encapsulating mobile proton carriers into structural defects in coordination polymer crystals: High anhydrous proton conduction and fuel cell application. *J. Am. Chem. Soc.* **138**, 8505–8511 (2016).
69. K. Fujie, R. Ikeda, K. Otsubo, T. Yamada, H. Kitagawa, Lithium ion diffusion in a metal–organic framework mediated by an ionic liquid. *Chem. Mater.* **27**, 7355–7361 (2015).
70. R. Ameloot, M. Aubrey, B. M. Wiers, A. P. Gómora-Figueroa, S. N. Patel, N. P. Balsara, J. R. Long, Ionic conductivity in the metal–organic framework UiO-66 by dehydration and insertion of lithium *tert*-butoxide. *Chem. Eur. J.* **19**, 5533–5536 (2013).
71. B. M. Wiers, M.-L. Foo, N. P. Balsara, J. R. Long, A solid lithium electrolyte via addition of lithium isopropoxide to a metal–organic framework with open metal sites. *J. Am. Chem. Soc.* **133**, 14522–14525 (2011).
72. M. L. Aubrey, R. Ameloot, B. M. Wiers, J. R. Long, Metal–organic frameworks as solid magnesium electrolytes. *Energy Environ. Sci.* **7**, 667–671 (2014).
73. M. Hu, J. Reboul, S. Furukawa, N. L. Torad, Q. Ji, P. Srinivasu, K. Ariga, S. Kitagawa, Y. Yamauchi, Direct carbonization of Al-based porous coordination polymer for synthesis of nanoporous carbon. *J. Am. Chem. Soc.* **134**, 2864–2867 (2012).
74. H.-L. Jiang, B. Liu, Y.-Q. Lan, K. Kuratani, T. Akita, H. Shioyama, F. Zong, Q. Xu, From metal–organic framework to nanoporous carbon: Toward a very high surface area and hydrogen uptake. *J. Am. Chem. Soc.* **133**, 11854–11857 (2011).
75. P. Pachfule, D. Shinde, M. Majumder, Q. Xu, Fabrication of carbon nanorods and graphene nanoribbons from a metal–organic framework. *Nat. Chem.* **8**, 718–724 (2016).
76. F. Zheng, Y. Yang, Q. Chen, High lithium anodic performance of highly nitrogen-doped porous carbon prepared from a metal-organic framework. *Nat. Commun.* **5**, 5261 (2014).
77. S. Gadipelli, T. Zhao, S. A. Shevlin, Z. Guo, Switching effective oxygen reduction and evolution performance by controlled graphitization of a cobalt–nitrogen–carbon framework system. *Energy Environ. Sci.* **9**, 1661–1667 (2016).

78. J. Tang, R. R. Salunkhe, J. Liu, N. L. Torad, M. Imura, S. Furukawa, Y. Yamauchi, Thermal conversion of core–shell metal–organic frameworks: A new method for selectively functionalized nanoporous hybrid carbon. *J. Am. Chem. Soc.* **137**, 1572–1580 (2015).
79. R. R. Salunkhe, J. Tang, Y. Kamachi, T. Nakato, J. H. Kim, Y. Yamauchi, Asymmetric supercapacitors using 3D nanoporous carbon and cobalt oxide electrodes synthesized from a single metal–organic framework. *ACS Nano* **9**, 6288–6296 (2015).
80. L. Zhang, H. B. Wu, S. Madhavi, H. H. Hng, X. W. Lou, Formation of Fe_2O_3 microboxes with hierarchical shell structures from metal–organic frameworks and their lithium storage properties. *J. Am. Chem. Soc.* **134**, 17388–17391 (2012).
81. W. Cho, S. Park, M. Oh, Coordination polymer nanorods of Fe-MIL-88B and their utilization for selective preparation of hematite and magnetite nanorods. *Chem. Commun.* **47**, 4138–4140 (2011).
82. B. Y. Xia, Y. Yan, N. Li, H. B. Wu, X. W. Lou, X. Wang, A metal–organic framework-derived bifunctional oxygen electrocatalyst. *Nat. Energy* **1**, 15006 (2016).
83. A. Aijaz, J. Masa, C. Rösler, W. Xia, P. Weide, A. J. R. Botz, R. A. Fischer, W. Schuhmann, M. Muhler, Co@Co_3O_4 encapsulated in carbon nanotube-grafted nitrogen-doped carbon polyhedra as an advanced bifunctional oxygen electrode. *Angew. Chem. Int. Ed.* **55**, 4087–4091 (2016).
84. B. Y. Guan, L. Yu, X. W. Lou, A dual-metal–organic-framework derived electrocatalyst for oxygen reduction. *Energy Environ. Sci.* **9**, 3092–3096 (2016).
85. F. Zou, X. Hu, Z. Li, L. Qie, C. Hu, R. Zeng, Y. Jiang, Y. Huang, MOF-derived porous ZnO/$ZnFe_2O_4$/C octahedra with hollow interiors for high-rate lithium-ion batteries. *Adv. Mater.* **26**, 6622–6628 (2014).
86. S. J. Yang, S. Nam, T. Kim, J. H. Im, H. Jung, J. H. Kang, S. Wi, B. Park, C. R. Park, Preparation and exceptional lithium anodic performance of porous carbon-coated ZnO quantum dots derived from a metal–organic framework. *J. Am. Chem. Soc.* **135**, 7394–7397 (2013).
87. P. Yin, T. Yao, Y. Wu, L. Zheng, Y. Lin, W. Liu, H. Ju, J. Zhu, X. Hong, Z. Deng, G. Zhou, S. Wei, Y. Li, Single cobalt atoms with precise N-coordination as superior oxygen reduction reaction catalysts. *Angew. Chem. Int. Ed.* **55**, 10800–10805 (2016).
88. H. Zhang, T. Wang, J. Wang, H. Liu, T. D. Dao, M. Li, G. Liu, X. Meng, K. Chang, L. Shi, T. Nagao, J. Ye, Surface-plasmon-enhanced photodriven CO_2 reduction catalyzed by metal–organic-framework-derived iron nanoparticles encapsulated by ultrathin carbon layers. *Adv. Mater.* **28**, 3703–3710 (2016).
89. Y. Hou, Z. Wen, S. Cui, S. Ci, S. Mao, J. Chen, An advanced nitrogen-doped graphene/cobalt-embedded porous carbon polyhedron hybrid for efficient catalysis of oxygen reduction and water splitting. *Adv. Funct. Mater.* **25**, 872–882 (2015).
90. L. Zhang, H. B. Wu, X. W. Lou, Metal–organic-frameworks-derived general formation of hollow structures with high complexity. *J. Am. Chem. Soc.* **135**, 10664–10672 (2013).
91. J. Zhang, H. Hu, Z. Li, X. W. Lou, Double-shelled nanocages with cobalt hydroxide inner shell and layered double hydroxides outer shell as high-efficiency polysulfide mediator for lithium–sulfur batteries. *Angew. Chem. Int. Ed.* **55**, 3982–3986 (2016).
92. X.-Y. Yu, L. Yu, H. B. Wu, X. W. Lou, Formation of nickel sulfide nanoframes from metal–organic frameworks with enhanced pseudocapacitive and electrocatalytic properties. *Angew. Chem. Int. Ed.* **54**, 5331–5335 (2015).
93. P. Zhang, B. Y. Guan, L. Yu, X. W. Lou, Formation of double-shelled zinc–cobalt sulfide dodecahedral cages from bimetallic zeolitic imidazolate frameworks for hybrid supercapacitors. *Angew. Chem. Int. Ed.* **56**, 7141–7145 (2017).
94. K. Cho, S.-H. Han, M. P. Suh, Copper–organic framework fabricated with CuS nanoparticles: Synthesis, electrical conductivity, and electrocatalytic activities for oxygen reduction reaction. *Angew. Chem. Int. Ed.* **55**, 15301–15305 (2016).
95. H. Hu, J. Zhang, B. Guan, X. W. Lou, Unusual formation of CoSe@carbon nanoboxes, which have an inhomogeneous shell, for efficient lithium storage. *Angew. Chem. Int. Ed.* **55**, 9514–9518 (2016).
96. X.-Y. Yu, Y. Feng, B. Guan, X. W. Lou, U. Paik, Carbon coated porous nickel phosphides nanoplates for highly efficient oxygen evolution reaction. *Energy Environ. Sci.* **9**, 1246–1250 (2016).
97. P. He, X.-Y. Yu, X. W. Lou, Carbon-incorporated nickel–cobalt mixed metal phosphide nanoboxes with enhanced electrocatalytic activity for oxygen evolution. *Angew. Chem. Int. Ed.* **56**, 3897–3900 (2017).
98. R. Bendi, V. Kumar, V. Bhavanasi, K. Parida, P. S. Lee, Metal organic framework-derived metal phosphates as electrode materials for supercapacitors. *Adv. Energy Mater.* **6**, 1501833 (2016).
99. W. Guo, W. Xia, K. Cai, Y. Wu, B. Qiu, Z. Liang, C. Qu, R. Zou, Kinetic-controlled formation of bimetallic metal–organic framework hybrid structures. *Small* **2017**, 1702049 (2017).
100. X. Song, T. K. Kim, H. Kim, D. Kim, S. Jeong, H. R. Moon, M. S. Lah, Post-synthetic modifications of framework metal ions in isostructural metal–organic frameworks: Core–shell heterostructures via selective transmetalations. *Chem. Mater.* **24**, 3065–3073 (2012).
101. C. R. Wade, M. Dincă, Investigation of the synthesis, activation, and isosteric heats of CO_2 adsorption of the isostructural series of metal–organic frameworks $M_3(BTC)_2$ (M = Cr, Fe, Ni, Cu, Mo, Ru). *Dalton Trans.* **41**, 7931–7938 (2012).
102. H. B. Wu, B. Y. Xia, L. Yu, X.-Y. Yu, X. W. Lou, Porous molybdenum carbide nano-octahedrons synthesized via confined carburization in metal-organic frameworks for efficient hydrogen production. *Nat. Commun.* **6**, 6512 (2015).
103. Y.-J. Tang, M.-R. Gao, C.-H. Liu, S.-L. Li, H.-L. Jiang, Y.-Q. Lan, M. Han, S.-H. Yu, Porous molybdenum-based hybrid catalysts for highly efficient hydrogen evolution. *Angew. Chem. Int. Ed.* **54**, 12928–12932 (2015).
104. Y. Chen, S. Ji, Y. Wang, J. Dong, W. Chen, Z. Li, R. Shen, L. Zheng, Z. Zhuang, D. Wang, Y. Li, Isolated single iron atoms anchored on N-doped porous carbon as an efficient electrocatalyst for the oxygen reduction reaction. *Angew. Chem. Int. Ed.* **56**, 6937–6941 (2017).
105. Q. Li, P. Xu, W. Gao, S. Ma, G. Zhang, R. Cao, J. Cho, H.-L. Wang, G. Wu, Graphene/graphene-tube nanocomposites templated from cage-containing metal-organic frameworks for oxygen reduction in Li–O_2 batteries. *Adv. Mater.* **26**, 1378–1386 (2014).
106. K. Strickland, E. Miner, Q. Jia, U. Tylus, N. Ramaswamy, W. Liang, M.-T. Sougrati, F. Jaouen, S. Mukerjee, Highly active oxygen reduction non-platinum group metal electrocatalyst without direct metal–nitrogen coordination. *Nat. Commun.* **6**, 7343 (2015).
107. G. Lu, S. Li, Z. Guo, O. K. Farha, B. G. Hauser, X. Qi, Y. Wang, X. Wang, S. Han, X. Liu, J. S. DuChene, H. Zhang, Q. Zhang, X. Chen, J. Ma, S. C. J. Loo, W. D. Wei, Y. Yang, J. T. Hupp, F. Huo, Imparting functionality to a metal–organic framework material by controlled nanoparticle encapsulation. *Nat. Chem.* **4**, 310–316 (2012).
108. Y. V. Kaneti, S. Dutta, S. A. Hossain, M. J. A. Shiddiky, K.-L. Tung, F.-K. Shieh, C.-K. Tsung, K. C.-W. Wu, Y. Yamauchi, Strategies for improving the functionality of zeolitic imidazolate frameworks: Tailoring nanoarchitectures for functional applications. *Adv. Mater.* **29**, 1700213 (2017).
109. X. Xu, R. Cao, S. Jeong, J. Cho, Spindle-like mesoporous α-Fe_2O_3 anode material prepared from MOF template for high-rate lithium batteries. *Nano Lett.* **12**, 4988–4991 (2012).
110. Y. Yang, Z. Lun, G. Xia, F. Zheng, M. He, Q. Chen, Non-precious alloy encapsulated in nitrogen-doped graphene layers derived from MOFs as an active and durable hydrogen evolution reaction catalyst. *Energy Environ. Sci.* **8**, 3563–3571 (2015).
111. L. Han, X.-Y. Yu, X. W. Lou, Formation of Prussian-blue-analog nanocages via a direct etching method and their conversion into Ni–Co-mixed oxide for enhanced oxygen evolution. *Adv. Mater.* **28**, 4601–4605 (2016).
112. H. Hu, B. Guan, B. Xia, X. W. Lou, Designed formation of Co_3O_4/$NiCo_2O_4$ double-shelled nanocages with enhanced pseudocapacitive and electrocatalytic properties. *J. Am. Chem. Soc.* **137**, 5590–5595 (2015).
113. W. Xia, R. Zou, L. An, D. Xia, S. Guo, A metal–organic framework route to in situ encapsulation of Co@Co_3O_4@C core@bishell nanoparticles into a highly ordered porous carbon matrix for oxygen reduction. *Energy Environ. Sci.* **8**, 568–576 (2015).
114. H.-x. Zhong, J. Wang, Y.-w. Zhang, W.-l. Xu, W. Xing, D. Xu, Y.-f. Zhang, X.-b. Zhang, ZIF-8 derived graphene-based nitrogen-doped porous carbon sheets as highly efficient and durable oxygen reduction electrocatalysts. *Angew. Chem. Int. Ed.* **53**, 14235–14239 (2014).
115. Z. Li, M. Shao, L. Zhou, R. Zhang, C. Zhang, M. Wei, D. G. Evans, X. Duan, Directed growth of metal-organic frameworks and their derived carbon-based network for efficient electrocatalytic oxygen reduction. *Adv. Mater.* **28**, 2337–2344 (2016).
116. Y. M. Chen, L. Yu, X. W. Lou, Hierarchical tubular structures composed of Co_3O_4 hollow nanoparticles and carbon nanotubes for lithium storage. *Angew. Chem. Int. Ed.* **55**, 5990–5993 (2016).
117. X. Cao, B. Zheng, X. Rui, W. Shi, Q. Yan, H. Zhang, Metal oxide-coated three-dimensional graphene prepared by the use of metal–organic frameworks as precursors. *Angew. Chem. Int. Ed.* **53**, 1404–1409 (2014).
118. T. Y. Ma, S. Dai, M. Jaroniec, S. Z. Qiao, Metal–organic framework derived hybrid Co_3O_4-carbon porous nanowire arrays as reversible oxygen evolution electrodes. *J. Am. Chem. Soc.* **136**, 13925–13931 (2014).
119. G. Zhang, S. Hou, H. Zhang, W. Zeng, F. Yan, C. C. Li, H. Duan, High-performance and ultra-stable lithium-ion batteries based on MOF-derived ZnO@ZnO quantum dots/C core–shell nanorod arrays on a carbon cloth anode. *Adv. Mater.* **27**, 2400–2405 (2015).
120. W. Xia, C. Qu, Z. Liang, B. Zhao, S. Dai, B. Qiu, Y. Jiao, Q. Zhang, X. Huang, W. Guo, D. Dang, R. Zou, D. Xia, Q. Xu, M. Liu, High-performance energy storage and conversion materials derived from a single metal–organic framework/graphene aerogel composite. *Nano Lett.* **17**, 2788–2795 (2017).
121. W. Xia, B. Qiu, D. Xia, R. Zou, Facile preparation of hierarchically porous carbons from metal-organic gels and their application in energy storage. *Sci. Rep.* **3**, 1935 (2013).

122. A. J. Amali, J.-K. Sun, Q. Xu, From assembled metal–organic framework nanoparticles to hierarchically porous carbon for electrochemical energy storage. *Chem. Commun.* **50**, 1519–1522 (2014).
123. L. Yu, H. B. Wu, X. W. Lou, Self-templated formation of hollow structures for electrochemical energy applications. *Acc. Chem. Res.* **50**, 293–301 (2017).
124. B. Y. Guan, A. Kushima, L. Yu, S. Li, J. Li, X. W. Lou, Coordination polymers derived general synthesis of multishelled mixed metal-oxide particles for hybrid supercapacitors. *Adv. Mater.* **29**, 1605902 (2017).
125. B. Y. Guan, L. Yu, X. Wang, S. Song, X. W. Lou, Formation of onion-like $NiCo_2S_4$ particles via sequential ion-exchange for hybrid supercapacitors. *Adv. Mater.* **29**, 1605051 (2017).
126. K. Xi, S. Cao, X. Peng, C. Ducati, R. V. Kumar, A. K. Cheetham, Carbon with hierarchical pores from carbonized metal-organic frameworks for lithium sulphur batteries. *Chem. Commun.* **49**, 2192–2194 (2013).
127. H. B. Wu, S. Wei, L. Zhang, R. Xu, H. H. Hng, X. W. Lou, Embedding sulfur in MOF-derived microporous carbon polyhedrons for lithium–sulfur batteries. *Chem. Eur. J.* **19**, 10804–10808 (2013).
128. Z. Li, H. B. Wu, X. W. Lou, Rational designs and engineering of hollow micro-/nanostructures as sulfur hosts for advanced lithium–sulfur batteries. *Energy Environ. Sci.* **9**, 3061–3070 (2016).
129. Z.-F. Huang, J. Song, K. Li, M. Tahir, Y.-T. Wang, L. Pan, L. Wang, X. Zhang, J.-J. Zou, Hollow cobalt-based bimetallic sulfide polyhedra for efficient all-pH-value electrochemical and photocatalytic hydrogen evolution. *J. Am. Chem. Soc.* **138**, 1359–1365 (2016).
130. D. Zhao, J.-L. Shui, L. R. Grabstanowicz, C. Chen, S. M. Commet, T. Xu, J. Lu, D.-J. Liu, Highly efficient non-precious metal electrocatalysts prepared from one-pot synthesized zeolitic imidazolate frameworks. *Adv. Mater.* **26**, 1093–1097 (2014).
131. M. Gaab, N. Trukhan, S. Maurer, R. Gummaraju, U. Müller, The progression of Al-based metal-organic frameworks—From academic research to industrial production and applications. *Microporous Mesoporous Mater.* **157**, 131–136 (2012).

Acknowledgments
Funding: H.B.W. acknowledges start-up funding support from Zhejiang University and the Thousand Young Talents Program of China. X.W.L. acknowledges the funding support from the National Research Foundation (NRF) of Singapore via the NRF investigatorship (NRF-NRFI2016-04). **Author contributions:** H.B.W. and X.W.L. co-wrote the manuscript. **Competing interests:** The authors declare that they have no competing interests. **Data and materials availability:** All data needed to evaluate the conclusions in the paper are present in the articles cited herein.

Submitted 11 September 2017
Accepted 24 October 2017
Published 1 December 2017
10.1126/sciadv.aap9252

Citation: H. B. Wu, X. W. Lou, Metal-organic frameworks and their derived materials for electrochemical energy storage and conversion: Promises and challenges. *Sci. Adv.* **3**, eaap9252 (2017).